Letter of reply and track-changes manuscript for BG-2019-286.

Dear Prof. Luyssaert, Dear reviewers,

Thank you very much for considering our manuscript for publication and the constructive feedback on our initial submission. We have now thoroughly revised our manuscript 'Quantifying impacts of the drought 2018 on European ecosystems in comparison to 2003' in light of the interactive discussion'. Major changes undertaken in course of the revision are:

- Adding spatiotemporal analyses of climate and remote sensing data (including four supplementary videos), to depict the differing temporal development of the two drought events
- Changed the comparison between 2003 and 2018 to now emphasize on the peak of drought in both years, i.e. August 2003 vs. July 2018.
- Elaborated the methods and discussion sections to clarify potential ambiguity and strengthen the discussion on the spatiotemporal differences of drought impacts.

As can be seen in the revised document, the general message of the study – which was in parts challenged by the reviewers – remains consistent, namely that the drought 2018 superseded the one of 2003 both with regard to climatic features but also ecosystem response. The added analyses provide more insight into the development of the two differing droughts. Refined discussions on the differences and hypotheses for their explanation now more clearly stimulate research questions for future studies. We are therefore confident, that our revision and reply addresses all of the points raised by the reviewers which helped us to significantly improve our manuscript, even if we did not incorporate all of the reviewer's suggestions for reasons that are explained in our point-by-point reply below. We therefore hope that these amendments justify publication in *Biogeosciences.*

Please find our point by point reply (your comments in normal font, ours in italics with text citations in bold) as well as the track-changes document of our revision below.

Anonymous Referee #1

Received and published: 19 August 2019

In this manuscript, the authors compare the climatological features of two intense drought events over Europe, the 2003 and 2018 heatwaves. From a climatological analysis, they carry on to analyze the effect of both events on European vegetation. The authors' results are based on a suite of statistical analyses of MODIS-based vegetation indices combined with a widely used land cover map. Their main conclusion is that the 2018 heatwave had a stronger effect on European vegetation than the 2003 one.

General comments

Overall the manuscript is well written and follows a logic questioning line going from the climatology of the heatwave to the effect on vegetation. However, I am not convinced by the relevancy of the way the main question is addressed. From the first climatological data shown by the authors it is obvious that the 2003 and 2018 events are very different in terms of location (baltic countries in 2018 versus central Europe in 2003) and timing (july was the beginning of the 2003 heatwave whereas it was the end of the 2018 one) and, even though it is not shown, in initial conditions. These crucial differences are however mostly ignored in the way the analyses are designed, potentially pointing to severe flaws in the results, that I detail below. This observation leads me to suggest more detailed analyses be carried out before publication.

Thank you very much for your constructive review which highlights important aspects and potential ambiguities that made us improve our analyses and consequently the manuscript. Major changes to the manuscript in light of your comments are:

1) *Visualizing the spatiotemporal development of climatic conditions using time-series and animated videos (Fig. S5 and supplementary videos V1 and V2* http://doi.org/10.5446/44027 and http://doi.org/10.5446/44028*) to better quantify the climatic conditions of the two events,*
2) *Provide further supplementary videos (V3 and V4* http://doi.org/10.5446/44029 and http://doi.org/10.5446/44030*) which visualize the temporal development of NDVI and EVI quantiles using maps and histograms (as in Fig. 4) from beginning of May until end of October to allow for assessing the temporal development of ecosystem response to the two drought events,*
3) *Comparing and modelling the ecosystem response representative of the peak of drought in each year (i.e. DOY 209 in 2018 vs. DOY 241 in 2003) instead of for DOY 209,*
4) *Elaborating the discussion regarding the outlined spatiotemporal effects.*

All of these additional analyses confirm the initial impression that the drought 2018 was more severe compared to 2003. However, we now pay more attention to outline the different spatial impact and timing of the drought 2018 compared to 2003 which is related to the more northward location of the drought center. Please find our more detailed responses below.

Detailed comments

Effect of heatwave timing, duration and legacy

The analyses carried out, only encompassing the greenness index in july of both years, seem too superficial to draw the far-reaching conclusions the authors make. First on heatwave timing, the stronger NDVI signal in july 2018 compared to july 2003 could be the result of the difference in timing. This point is ignored when concluding that the 2018 heatwave had a stronger effect on European ecosystems than the 2003 one.

We agree that the different timing of the drought and heatwaves likely resulted in a different timing of vegetation response. To better visualize the observed temporal development, we added supplementary videos which depict the temporal development of NDVI and EVI from beginning of May until end of October (supplementary videos V3 and V4). Moreover, we added time-series comparable to those shown in Fig. 6 for TMAX and CWB to provide a direct comparison between the climatic features of the drought affected areas in 2003 and 2018 (Fig. S5) as well as videos depicting the course of TMAX and CWB from January through October for both years (V1 and V2). These results further strengthen our initial conclusion that the 2018 event overall had a larger extent and a stronger effect on European ecosystems compared to 2003. In our revision we have pointed out more clearly the differences between the timing and location of drought, i.e. we added several paragraphs to the discussion about the additional analyses and the importance of drought timing and location, for example in

Line 347: ***Moreover, the two drought events differed regarding their timing and location, with 2018 featuring an earlier peak of drought (July vs. August in 2003) and a more northward centre around the Baltic Sea vs. the Mediterranean in 2003.***

Line 425: ***The earlier timing possibly also triggered a stronger response to the drought in 2018, particularly in Northern Europe where it began as early as May, i.e. at the beginning of the growing season (Fig. S5 and V2). Northern European forests are dominated by coniferous forests that to a large degree consist of Norway spruce and Scots pine, i.e. two tree species that have been frequently reported to suffer under drought (e.g. Buras et al., 2018; Kohler et al., 2010; Rehschuh et al., 2017; Rigling et al., 2013). Moreover, coniferous forests made up a high share of the drought affected ecosystems in 2018 (Fig. S6). In combination, the potentially stronger reaction of high latitude coniferous forests may partly explain the observed stronger coupling between CWB anomalies and VI quantiles in 2018 compared to 2003.***

Second, as mentioned as a discussion item, the legacy of water balance can be very important for heatwave effects on forests especially. Even though this is be a major point underlying the relevancy of the question asked, no data or analysis shown tries to compare the water conditions prior to both heatwaves. An analysis of both heatwaves time evolution and the comparison of each heatwave's end month, that could then be different from one to the other could be an option.

We agree that the water balance legacy effects are relevant, wherefore we added analyses to the manuscript that address this issue. In particular, we visualized the development of integrated CWB over time, i.e. including preceding winter conditions and extending until the end of the growing season (Fig.

S5) and added corresponding supplementary videos (V1 and V2). We acknowledge your suggestion to compare different months with each other. We now compare VI quantiles representing DOY 241 in 2003 and DOY 209 in 2018 in Figs. 4 and 5, and use the corresponding VI-quantiles and CWB for the modelling exercise presented in Fig. 7 and the mixed model. Having added these analyses to the manuscript now provides a more comprehensive picture of the difference between the two drought events.

Heatwave location defining the ecosystems affected

Another point that undermines the results presented is the comparison of vegetation types in absolute terms without a prior description of vegetation types affected in each case that might be very different. Even though this information is essential to make sense of a comparison of the effects on vegetation of two climatic events, it is hardly discussed and made very hard to see in the way the data are processed. For example the varying y-axis ranges in figure
5 hide the relative weights of each vegetation type with water deficit or water surplus.
Figure S3 might be more explicit to this regard by considering relative vegetation cover.

Maybe we misunderstood your comment, but we struggle to reproduce your statement that the effects of the different locations of the drought are 'hardly discussed'. Section 4.2.2 particularly deals with the possible effect of the differing drought epicenters, where we highlight that the different ecosystems' adaptation to drought likely caused the stronger ecosystem response in 2018. To account for your critique, we have added Fig. S6 which depicts the share of ecosystems that were affected by the two drought events, respectively. This figure further highlights the fact that the drought-affected areas differ between 2003 and 2018, which leads to varying absolute areas as well as different vegetation types that were affected. However, given the nature of the data available for land-cover classification, it is not possible to differentiate these classes further. We are aware that this is associated with potential problems, a fact that we recommend to take into consideration in follow-up studies. Moreover, we now emphasize the potentially stronger response of high latitude coniferous forests in comparison to Mediterranean forests. Please see the two text excerpts from chapter 4.2.2 below:

Line 426: Northern European forests are dominated by coniferous forests that to a large degree consist of Norway spruce and Scots pine, i.e. two tree species that have been frequently reported to suffer from drought (e.g. Buras et al., 2018; Kohler et al., 2010; Rehschuh et al., 2017; Rigling et al., 2013). Moreover, coniferous forests made up a high share of the drought affected ecosystems in 2018 (Fig. S6). In combination, the potentially stronger reaction of high latitude coniferous forests may partly explain the observed stronger coupling between CWB anomalies and VI quantiles in 2018 compared to 2003.

Line 439: Nevertheless, our hypotheses explaining the stronger coupling of VI quantiles with CWB in 2018 need further support, e.g. by studying the sensitivity and coupling of plant productivity with climatic properties for the considered land-cover classes as for instance done by (Anderegg et al., 2018). A sub-classification of land-cover classes seems to be reasonable for such an analysis, in order to account for possibly differing drought-

sensitivities of ecosystems represented by one specific land-cover class. For instance, Mediterranean coniferous forests comprise different species and are thus likely better adapted to drought than boreal coniferous forests in Scandinavia.

Also, we would like to emphasize the importance of Fig. 5 for the main aim of the paper, i.e. to compare 2003 with 2018. This figure fulfills two different tasks. On the one hand, we use it to show the absolute areas of drought affected ecosystems but separated by land-cover type. On the other hand, we use Fig. 5 to visualize how the quantiles are distributed within the 3 different classes of CWB-anomalies which indicates the effect of CWB on quantile-distributions. We are therefore convinced, that Fig. 5 provides an important message, namely that the area featuring extreme drought (CWB <-2) was larger in 2018 (already mentioned in the results of CWB anomalies but now also shown in Fig. S6) but that this higher area was unevenly distributed among the different vegetation types. For instance, while coniferous and mixed forests reveal a much larger spatial area featuring lowest VI-quantiles in 2018 compared to 2003, broadleaved forests revealed opposite patterns, i.e. a larger area of lowest quantiles in 2003.

We agree, that information is also needed on the relative contribution of each land-cover type to the drought affected areas, which is the reason why we also supplied Fig. S3 (now Fig. S8) and report the corresponding results in the results section. However, since the main emphasis of the paper is to compare the absolute drought effects, histograms relying on absolute areas are mandatory.

Statistical indices

Finally, another aspect of the manuscript that makes it less convincing is the choice of the figures and complex statistical indices derived. For example figure 5 is hard to interprete. What is the implication of high NDVIs combined with low CWB? In general, the methods section is very concise, making it easy to read but also lacking some key points to help the reader understand the many indices used. For example even though they are widely used NDVI and EVI should be defined. Also, heat load variable is not defined and is sometimes written heat load and sometimes heat-load. If it is simply Tmax call it this.

We agree that the methods should be sufficiently precise to enable reproducing the analyses, and have added mathematical definitions of NDVI and EVI and generally elaborated the methods section to better explain what we did and why we did this. According to the reviewers' suggestion, we renamed heat load to Tmax.

However, we disagree with your statement regarding the application of complex statistical indices. In fact, many of the applied statistics are rather simple, i.e. transformation of processed values into anomalies (a simple z-transformation) and quantiles (a simple ranking) and then providing mostly descriptive statistics. Moreover, we show simple ordinary linear regressions between NDVI-quantiles

and CWB. The only more complex statistical approach is related to the mixed-effects model, which however, after being introduced in 1918, is becoming more and more common in environmental sciences.

As mentioned in the reply to your previous comment, Fig. 5 serves two tasks, i.e. 1) highlighting the much higher area of affected ecosystems with a different distribution among land-cover types and 2) exemplifying the effect of CWB on the distribution of quantiles. Under normal conditions, quantiles will express a uniform distribution, while a skewed distribution indicates abnormal conditions, such as for the classes with CWB < -2 and CWB > 0. Showing the skewed quantile distributions directly leads to the modelling exercises shown in Fig. 7.

The outlined amount of combinations with high NDVI but low CWB is relatively low and much lower than expected if assuming a uniform quantile-distribution due to the significant impact of CWB-deficit on NDVI quantiles. The reason for why we yet observe high NDVI-values despite low CWB is likely related to the different spatial resolutions of the used products, i.e. climate data with 0.5° resolution and satellite data with 231 m resolution. That is, within one climate grid cell elevational differences and variations in groundwater levels (e.g. along rivers or lake shores) may modify the vegetation response to gridded CWB, since the coarse resolution of the climate data neither capture small-scale climatic variations due to elevation nor represent groundwater levels. We have added two corresponding paragraphs to chapter 4.2.1 of the discussion to make this clearer:

Line 384: We want to note that we also observed small areas (ca. 1000 km² for each of the considered land cover classes) of high quantiles in regions featuring extreme drought. This observation is likely related to the different resolution of climate data (0.5°, thus ca. 50 km x 50 km) vs. MODIS (231 m x 231 m). Using such relatively coarse climate data for quantifying drought neglects elevation-driven climatic variations within grid cells (Zang et al., 2019) in contrast to the relatively higher resolution of MODIS which likely captures such differences. For instance, mountain ranges – which on average feature cooler temperatures (thus less evapotranspiration) and higher precipitation – likely feature less extreme water deficit compared to surrounding lowlands which may cause higher VI values than one would expect if only considering the drought classification of the corresponding climate grid cell. In addition, groundwater availability – which may vary within climate grid cells, particularly in proximity to rivers and lakes – may locally modulate plant water availability, possibly explaining some of the observations of high VI quantiles under extreme drought.

Line 394: Furthermore, quantifying drought on anomalies alone bears the risk to erroneously classify regions that actually feature water surplus (CWB > 0) as being drought-affected (Zang et al., 2019). This is likely to happen in regions which usually have high water surplus (e.g. the Norwegian west-coast) and thus may feature more than two negative CWB standard deviations even though raw CWB is positive (Zang et al., 2019). For both 2003 and 2018, 5 (1) percent of climate grid cells featured positive CWB even though CWB anomalies indicated

(extreme) water deficit (CWB < 0 and CWB < -2 SD, see also Fig. S13). This false classification may explain some of the observed highest quantiles in regions that were classified as featuring extreme water deficit. Since we currently lack a more advanced drought-metric that compensates for such effects, we followed the commonly applied approach and used standardized CWB for our analyses. To show the full picture, we at the same identify potential biases caused by this approach (Fig. S13) as proposed by Zang et al. (2019). Given the relatively low number of 'false' extreme drought classifications (1 percent for each year) we estimate the impact on our analyses to be generally low.

Anonymous Referee #2

Received and published: 9 September 2019

This is a well-written study comparing the European heatwaves of 2003 and 2018. Comparison of climatological data and vegetation indices lead to the conclusion that the 2018 heatwave was more severe than the 2003 heatwave. However, substantial regional differences occur. The idea behind this study is interesting, but the study misses out on several aspects needed to support the conclusions. Especially the lack of the temporal patterns in weather data makes it hard to evaluate the results. No time series for temperature, precipitation or drought indices are shown to illustrate the heatwave patterns of both years. Moreover, end of July was chosen as the study period for the impact on vegetation, hence ignoring any change that took place in August (e.g. the massive forest fires in Portugal early August 2018).

Thank you for your constructive review. We agree with most of your comments and have modified our manuscript accordingly. Please find our detailed responses below.

Specific comments:

L 96ff: I suggest to simply argue that you focused on March-Oct because that is the period of interest for vegetation dynamics and leaving out winter helps avoiding artefacts (e.g. snow cover, but also defoliation in deciduous systems).

Thank you for this suggestion. We have modified the corresponding text accordingly:

However, since we were only interested in VI time series during the growing season, we only considered the period from beginning of March (DOY 64) to end of October (DOY 304) for the definition of valid pixels.

L 104-105: interpolation may create artefacts when searching for anomalies – especially when there are gaps during the drought episode under study. I suppose this is of minor importance for this study, because gaps are less likely during periods of drought (i.e., no clouds), but I wonder if the interpolation can be avoided. If not, the possibility for such artefacts should at least be discussed.

As you pointed out correctly, the likelihood of gaps is very low in 2003 and 2018 since large parts of Europe were free of clouds during these events. However, in 2018 the Mediterranean experienced above average precipitation, which may have resulted in higher cloud cover and thus missing values. To quantify the amount of missing values, we computed maps for 2003 and 2018 which show the number of gaps that were filled in each of the two seasons and added a corresponding paragraph to the methods section in which we state that given a low number of gaps for the majority of pixels the influence on our analyses is likely low:

Line 108: To visualize the potential influence of this gap-filling procedure, we provide Fig. S1 which depicts the number of gaps filled in 2003 and 2018. Since 2/3 of pixels rendered one or zero gaps, and 95 % rendered five or less gaps (i.e. less than one third of corresponding images missing, thus presumably sufficient data for meaningful interpolation) we assume any potential biases caused by the gap-filling procedure to be marginal.

L 119ff: NDVI and EVI are mainly greenness indicators. They may reflect photosynthesis, but not if photosynthesis changes without changing greenness. This is particularly relevant for drought. In this sense, EVI is better than NDVI (see Vicca et al 2016, Scientific Reports). I therefore advise to use the EVI results rather than the NDVI in this manuscript. It should also be clearly indicated what these VIs can reflect (and what not!). This is completely missing from the discussion of the current manuscript, but needs to be discussed (i.e., are we looking at green biomass/browning/defoliation. . . and what are the implications for e.g. legacy effects).

We agree, that EVI has certain advantages over NDVI regarding its ability to detect specific changes in GPP as in Vicca et al., 2016. However, the study by Vicca et al., 2016 focused on GPP-reduction where no defoliation or leaf-coloration was observed. In contrast, both in 2003 and 2018 early leaf shedding and coloration was observed (see also Fig. S14 regarding phenological analyses undertaken). The question which VI to use for drought indices is widely debated and depends on the purpose. For instance, Li et al. 2010 (in Procedia of Environmental Sciences) found stronger correlations between NDVI and field observations in comparison to EVI. Moreover, NDVI is usually more chlorophyll sensitive and mainly reflects the photosynthetic activity (which we were mainly interested in) while EVI is more responsive to canopy structural variations (see e.g. Huete et al., 2002). Also, in light of the findings by Vicca et al., 2016, it is hard to interpret the fact that the area with lowest quantiles was larger for NDVI compared to EVI (Fig. 4 compared to Fig. S 4). That is, if a non-visible drought-response would have been missed by NDVI, the areas indicating a severe drought response should be larger for EVI, which does not seem to be the case. Finally, all of the cited studies which monitored drought-impacts by means of remote sensing made use of NDVI (Anyamba and Tucker, 2012; Orth et al., 2016; Xu et al., 2011), wherefore focusing on NDVI makes our work more comparable against previous studies. Since we were aware from the beginning that the choice of VI matters, we included EVI in the supplementary to provide the full picture. We have elaborated the corresponding methods section as proposed and added a paragraph to the discussion about NDVI-EVI comparison and outline the possibility to also assess other remotely sensed indices such as the photochemical reflectance index and solar-induced fluorescence in future studies. We have added the following paragraphs in

Line 126: Both NDVI and EVI are considered as proxy for photosynthetic carbon fixation, and thus allow for assessing possible changes in productivity in dependence of environmental conditions (Huete et al., 2006; Myneni et al., 1995; Xu et al., 2011). NDVI has earlier been used in the context of drought monitoring (Anyamba and Tucker, 2012) and assessing impacts of drought on ecosystems on large scales (Orth et al., 2016; Xu et al., 2011). While NDVI relies on information derived from the red and near infrared spectra (see equation 1) EVI

additionally makes use of the blue spectrum (see equation 2) to reduce atmospheric disturbance and influence of the understory:

$$NDVI = \frac{NIR - RED}{NIR + RED} \quad (1)$$

$$EVI = G \cdot \frac{NIR - RED}{NIR + C_1 \cdot RED - C_2 \cdot BLUE + L} \quad (2)$$

With G being the gain factor, C_1 and C_2 being the spectrum-specific coefficients of the aerosol resistance term, and L the canopy background adjustment term (G = 2.5, C_1 = 6, C_2 = 7.5, L = 1 for MODIS EVI, see Huete et al., 2002). Given these definitions, NDVI is more chlorophyll sensitive, while EVI is more sensitive to canopy structural variations (Huete et al., 2002). Thus, NDVI is more likely to reflect changes in leaf coloration as for instance in course of premature leaf senescence under drought, whereas EVI may better reflect early leaf shedding. For reasons of simplicity and to render our results comparable to previous studies which all used NDVI, we focus on results derived from NDVI. To provide the full picture, results derived from EVI are shown in the supplementary information which generally confirm the results based on NDVI.

Line 405: Finally, we want to stress that the choice of VI used for quantification of the ecosystem response to drought matters. While Li et al. (2010) found stronger relationships and lower errors between NDVI and ground observations made in grasslands, shrublands and forest in comparison to EVI, Vicca et al. (2016) reported EVI to be more sensitive to reductions in GPP that were not reflected by leaf coloration or early leaf senescence. Given the ongoing discussion, we present results from both VIs which generally support each other (e.g. comparison between Figs. 4 and S7, Figs. 7 and S12) but focused on NDVI to make our contribution directly comparable to previous studies dealing with drought impacts on ecosystems (Anyamba and Tucker, 2012; Orth et al., 2016; Xu et al., 2011). To complement our VI-based assessment, future studies may consider the use of solar-induced fluorescence which is known to be more sensitive to terrestrial photosynthesis (Li et al., 2018) and/or the photochemical reflectance index (Vicca et al., 2016).

L 141-142: awkward phrasing: Subsequently, we for 2003 and 2018 determined . . . should be: Subsequently, we determined the difference between 2003 and 2018 for the respective metric. . .

Thank you for this suggestion. We have modified the corresponding text accordingly.

L149ff: the timing of the heatwaves should be demonstrated with data to justify the choice to focus on end of July. Time series of temperature and CWB for e.g. France, Germany (which suffered from the heat in both 2003 and 2018), or even for the different regions (N, W, S, Central Europe). How sensitive is your

analysis to the time choice? Are results similar if the analyses were repeated for end of August for example?

We agree, that the timing of drought as well as the location of the drought differs between 2003 and 2018. To better visualize the temporal development in 2018 and 2003 we have added supplementary videos V1-V4 (http://doi.org/10.5446/44027, http://doi.org/10.5446/44028, http://doi.org/10.5446/44029, http://doi.org/10.5446/44030) and Figs. S5 and S11 depicting the temporal development of TMAX, CWB, NDVI and EVI in the two years. Fig. 6 was particularly designed for this purpose, but we understand that we had to elaborate this part. We now also perform the analyses depicted in Fig. 5 and 7 on the basis of a different selection of time slices for 2003 (DOY 241) and 2018 (DOY 209) to account for the differing timing of the droughts and have elaborated the discussion about potential impacts of the differing spatiotemporal development of the two drought events:

Line 348:** **Moreover, the two drought events differed regarding their timing and location, with 2018 featuring an earlier peak of drought (July vs. August in 2003) and a more northward centre around the Baltic Sea vs. the Mediterranean in 2003.

Line 426:** **The earlier timing possibly also triggered a stronger response to the drought in 2018, particularly in Northern Europe where it began as early as May, i.e. at the beginning of the growing season (Fig. S5 and V2). Northern European forests are dominated by coniferous forests that to a large degree consist of Norway spruce and Scots pine, i.e. two tree species that have been frequently reported to suffer from drought (e.g. Buras et al., 2018; Kohler et al., 2010; Rehschuh et al., 2017; Rigling et al., 2013). Moreover, coniferous forests made up a high share of the drought affected ecosystems in 2018 (Fig. S6). In combination, the potentially stronger reaction of high latitude coniferous forests may partly explain the observed stronger coupling between CWB anomalies and VI quantiles in 2018 compared to 2003.

L 150-151: VIs cannot be lower than 0. (anomalies can)

Here, we disagree. Given the formulation of VIs in the numerator (NIR-RED)/(NIR+RED), VIs range from -1 to +1 and will become zero if the reflectance in the red spectrum is larger than in the NIR. Also, we want to point out that we were not using anomalies of VIs, since VIs have a bounded distribution. That is, instead we computed quantiles. All of this is described in section 2.2:

Line 177: To quantify the response of European ecosystems to the two drought events, we focused on end-of-August (DOY 241) and end-of-July (DOY 209) VI values for 2003 and 2018, respectively. The selection of these particular dates was based on the peak of climatological drought (see previous paragraph). Since VI features a bounded distribution (values between -1 and +1), we could not apply a standardization approach as for the climate variables. Therefore, we computed for each VI time series its end-of-July quantiles over the 19 years similar to Orth et al. (2016).

L 159: What was done with pixels where land cover changed between 2003 and 2018?
Was that even considered? (I don't think it will have a big impact on the analyses,
but it's worth a mention).

Thanks for this mention. We have updated our analyses to now only consider pixels which featured consistent land cover in 2000 and 2018. We have added supplementary Fig. S3 which depicts which pixels were used.

L191: 0.55 should be 55% I suppose.

Thanks for spotting the error. We have corrected it accordingly.

Fig.1: why was the timing April-July chosen for these figure? This is not motivated in the text I think a time series with weather data would be very helpful to evaluate this choice (see earlier comment). I noticed that this is briefly mentioned in the discussion (l. 320), but data are not shown. Please do show these data.

We have added supplementary videos V1 and V2 and Fig. S5 to our analyses which depict the spatiotemporal development of TMAX and CWB. Moreover, we now compared the VI-quantiles and corresponding integrated climate parameters for the peak of drought in each year, i.e. August 2003 vs. July 2018.

Fig.4: It is unclear where VI-deviations from the mean were significant. Please clarify, also in the text.

This seems to be a misunderstanding of the shown values. Since we used quantiles and not anomalies, it is not possible to derive p-values for the presented values. The reason for using quantiles instead of anomalies is mentioned in section 2.2 (see also reply to your previous comment).

l.240ff: A map with vegetation types is missing to illustrate where the different vegetation types occur and how the differences in impact for the different vegetation types correspond with the regional differences (e.g. Scandinavia being dominated by conifer forests).

Fig. S3 has been added for this purpose. It depicts which pixels were eventually used and also to which land-cover class they belong.

Fig.6: consider moving to appendix, adding instead a figure with time series for weather data.

We have kept Fig. 6 in the main part of the manuscript but have complemented it with Fig. S5 which depicts the temporal development of TMAX and CWB for Northern, Central, and Southern Europe.

L 251: Fig. 7 shows EVI, not NDVI. The text is about NDVI. (I suggest to focus on EVI for in the main document and move NDVI to appendix – see earlier comment).

Thank you for spotting an error in the axis labelling. Actually, Fig. 7 shows NDVI and not EVI (the same results for EVI are shown in the supplementary, Fig S12). Regarding your suggestion to focus on EVI, please see our detailed reply above.

L328ff: Portugal suffered from severe wildfires in 2018. This is not included in the analyses because the fires occurred mostly in August and the analyses are only for April-July. Other important events may be missed out because of the choice for April-July.

We have added supplementary videos which will allow for assessing the temporal development of NDVI and EVI and consequently to spot other possibly important events. However, given the large extent of the European map, the wildfires are hardly seen in these videos, i.e. a few pixels in Portugal turn red in August but the majority of pixels remains blue. Moreover, we believe that given their comparably low relative spatial extent (please don't get us wrong - we are aware that these fires were massive but in relation to all European forests rather contribute a lower proportion of forest area) it seems likely that the overall impact of these regional wildfires on our analyses is low. Since our main aim is to compare the overall impact of drought between 2003 and 2018, we would prefer to refrain from detailed mentions of single events. For instance, Sweden, Denmark, and Germany also suffered from massive forest fires in July 2018.

L 340ff: I suggest to include in this part of the discussion some text on the relationship between ecosystem types and climatic regions and how this may/may not influence the interpretation (see also earlier suggestion for figure addition).

In complementation to Fig. 5, we have added figure S6 to the supplementary depicting the spatial contributions of the landcover types to the drought-affected areas. In section 4.2.2 we elaborated the discussion how the different adaptation of affected ecosystems probably affects our results and interpretation, i.e. the observed stronger ecosystem response of 2018 is probably related to the fact that less adapted ecosystems were hit by the drought:

Line 427: Northern European forests are dominated by coniferous forests that to a large degree consist of Norway spruce and Scots pine, i.e. two tree species that have been frequently reported to suffer from drought (e.g. Buras et al., 2018; Kohler et al., 2010; Rehschuh et al., 2017; Rigling et al., 2013). Moreover, coniferous forests made up a high share of the drought affected ecosystems in 2018 (Fig. S6). In combination, the potentially stronger reaction of high latitude coniferous forests may partly explain the observed stronger coupling between CWB anomalies and VI quantiles in 2018 compared to 2003.

L358: public news references are not appropriate for this statement.

We agree and have added supplementary Fig. S. 14 which depicts the earlier timing of leaf senescence based on phenological data for Germany.

Quantifying impacts of the drought 2018 on European ecosystems in comparison to 2003

Allan Buras[1], Anja Rammig[1], Christian S. Zang[1]

[1]Land Surface Atmosphere Interactions, Technical University of Munich, TUM School of Life Sciences Weihenstephan, Hans-Carl-von-Carlowitz Platz 2, 85354 Freising, Germany.

Correspondence to: Allan Buras (allan@buras.eu)

Abstract. In recent decades, an increasing persistence of atmospheric circulation patterns has been observed. In the course of the associated long-lasting anticyclonic summer circulations, heat waves and drought spells often coincide, leading to so-called hotter droughts. Previous hotter droughts caused a decrease in agricultural yields and increase in tree mortality, and thus, had a remarkable effect on carbon budgets and negative economic impacts. Consequently, a quantification of ecosystem responses to hotter droughts and a better understanding of the underlying mechanisms is crucial. In this context, the European hotter drought of the year 2018 may be considered as a key event. As a first step towards the quantification of its causes and consequences, we here assess anomalies of atmospheric circulation patterns, ~~temperature loads~~maximum temperature, and climatic water balance as potential drivers of ecosystem responses which are quantified by remote sensing using the MODIS vegetation indices NDVI and EVI. To place the drought of 2018 within a climatological context, we compare its climatic features and remotely sensed ecosystem response with the extreme hot drought of 2003. 2018 was characterized by a climatic dipole, featuring extremely hot and dry weather conditions north of the Alps but comparably cool and moist conditions across large parts of the Mediterranean. Analysing ecosystem response of five dominant land-cover classes, we found significant positive effects of ~~April-July~~ climatic water balance on ecosystem ~~productivity~~VI response. Negative drought impacts appeared to affect a 1.5 times larger area and to be significantly stronger in July 2018 compared to August 2003, i.e. at the respective peak of drought. Moreover, we found a significantly higher sensitivity of pastures and arable land to climatic water balance compared to forests in both years. The stronger coupling and higher sensitivity of ecosystem response in 2018 we explain by the prevailing climatic dipole: while the generally water-limited ecosystems of the Mediterranean experienced above-average climatic water balance, the less drought-adapted ecosystems of Central and Northern Europe experienced a record hot drought. In conclusion, this study quantifies the drought of 2018 as a yet unprecedented event, outlines hotspots of drought-impacted areas in 2018 which should be given particular attention in follow-up studies, and provides valuable insights into the heterogeneous responses of the dominant European ecosystems to hotter drought.

1 Introduction

More frequent and longer-lasting heat waves are expected to occur with global warming (IPCC, 2014). If such heat waves coincide with low precipitation sums, so-called 'global-change type droughts' or 'hotter droughts' emerge (Allen et al., 2015; Breshears et al., 2005). In the course of hotter droughts, positive feedback loops related to a non-linearly amplified soil-water depletion through evapotranspiration (Seneviratne et al., 2010) further aggravate surface-temperature anomalies because of reduced latent cooling (Fischer et al., 2007). To emphasize this interdependence of heat and drought and improve projections of potential high-impact events, hotter droughts were recently classified as compound events (Zscheischler et al., 2018). Accounting for the interdependence of climatic drivers for drought, climate model projections generally indicate an increase in the likelihood of a hotter drought during the 21st century (Zscheischler and Seneviratne, 2017). Given the associated climatic properties, hotter droughts are more likely to occur under abnormally stable anticyclonic atmospheric circulation patterns which were recently shown to be connected with a hemisphere-wide wavenumber 7 circulation pattern (Kornhuber et al., 2019). Abnormally stable anticyclonic atmospheric circulation patterns and associated wavenumber 7 circulation patterns have expressed an increasing frequency over the past decades (Horton et al., 2015; Kornhuber et al., 2019).

Hotter droughts feature a wide range of negative impacts on managed and natural ecosystems, e.g. reduced productivity, as indicated by lower vegetation greenness using remote sensing data (Allen et al., 2015; Choat et al., 2018; Ciais et al., 2005; Orth et al., 2016; Xu et al., 2011). As a consequence, agricultural yields decline remarkably during hotter droughts while drought-induced tree mortality increases, with both effects leading to significant economic losses (Allen et al., 2010; Buras et al., 2018; Cailleret et al., 2017; Choat et al., 2018; Ciais et al., 2005; Matusick et al., 2018). Moreover, since gross primary productivity (GPP) decreases during hotter droughts, the resulting lower net carbon uptake may change ecosystems from carbon sinks into carbon sources (Ciais et al., 2005; Xu et al., 2011). However, the response to drought may vary among different land-cover types, particularly between grasslands and forests (Teuling et al., 2010; Wolf et al., 2013).

On the continental scale, the European heat wave of 2003 is to date considered as the most extreme compound event in Europe over the last century with various impacts on human health (increased mortality particularly in France), economy (decreased crop yield in agriculture and forestry), and ecosystems (reduced productivity, forest die-back, and an increased frequency of forest fires; Fink et al., 2004; García-Herrera et al., 2010). According to Ciais et al. (2005), GPP of European ecosystems was reduced by 30 percent in summer 2003 – a yet unprecedented reduction in Europe's primary productivity which resulted in an estimated net carbon release of 0.5 PG C yr^{-1}. Given the wide-ranging impacts, potential climate change feedback loops, and the increasing frequencies of circulation patterns initiating compound events it is pivotal to better understand and thus more

precisely predict the response of managed and natural ecosystems to hotter droughts (Horton et al., 2015; Pfleiderer and Coumou, 2018; Sippel et al., 2017; Zscheischler and Seneviratne, 2017).

In the context of an increased persistence of circulation patterns, the European drought of 2018 is of particular interest. In April 2018, a high-pressure system established over Central Europe and persisted almost continuously until mid of October, thereby causing a long-lasting drought spell and record temperatures in central and northern Europe. Despite preliminary reports in public news and the world-wide-web (see list of public news references), the direct impacts resulting from the 2018 drought are still unexplored. Consequently, we here quantify the impacts of the extreme drought of 2018 on European ecosystems in comparison to the extreme drought in the year 2003. Thereby, we 1) provide an estimate of European ecosystems immediate response to the drought 2018 in relation to 2003, 2) identify hotspots of extreme drought and associated ecosystem response, and 3) aim at an improved mechanistic understanding of the processes driving ecosystem responses to extreme drought events.

2 Material and Methods

2.1 Data sources and preparation

2.1.1 Climate data

To visualize the general circulation patterns in 2003 and 2018 we downloaded gridded reanalysis data representing 500 hPa geopotential height from the NCEP/NCAR Reanalysis project provided by the NOAA climate prediction center (Kalnay et al., 1996) available at the Earth System Research Laboratory (ESRL, https://www.esrl.noaa.gov/). The downloaded data cover the period 1981-2018 at a daily temporal resolution and a spatial resolution of 2.5°. As a representation of high-pressure persistence, we computed the mean geopotential height for each grid cell ~~and year for the period from 1st of April until 31st of July~~integrated over four months.

~~From ESRL, we furthermore downloaded reanalyzed (NCEP/NCAR), daily gridded mean minimum and maximum temperature (Tmin, Tmax) and precipitation (P) sums at 0.5° spatial resolution covering the period 1981-2018 (Kalnay et al., 1996).~~Considering temperature and precipitation, we downloaded interpolated, gridded, monthly minimum and maximum temperature means as well as monthly precipitation sums from the Climate Research Unit (CRU TS 4.01) covering the period 1901-2018 (Harris et al., 2014) and a at a spatial resolution of 0.5°. For reasons of consistency when standardizing the date, we constrained CRU data to the same period as for geopotential height, i.e. 1981-2018. These variables were used to compute potential evapotranspiration (PET, as defined by Hargreaves, 1994) and the climatic water balance (CWB = P-PET, Thornthwaite, 1948). As done for geopotential height, we for each grid cell and year integrated Tmax and CWB ~~for the period from 1st of April until 31st of July as~~ over a four month period as measures of ~~heat load~~maximum temperature and water balance. We decided to integrate over four months, since integrated values representative of peak season conditions (July and August) covered the majority of the growing season (i.e. April-July and May-August). Results based on different integration periods (e.g. 3 months, 5 months) did not differ substantially and generally confirmed results based on the four month period.

Processed climate data were spatially truncated to match the region considered for the MODIS satellite images (see next section) resulting in ~~2312~~ 2521 climate grid cells representing an area of roughly ~~5.9~~4.9 million km² and covering 38 years. To allow for combination with MODIS data throughout the analyses, processed climate data were re-projected to MODIS native projection using zonal means while retaining ~~a~~ the spatial resolution of 0.5°.

2.1.2 MODIS vegetation indices

Using the Application for Extracting and Exploring Analysis Ready Samples (AppEEARS; https://lpdaacsvc.cr.usgs.gov/appeears) we downloaded two MODIS vegetation indices (VI, i.e. the Normalized Difference Vegetation Index NDVI and the Enhanced Vegetation Index EVI) and the corresponding pixel reliability layers at 231 m spatial resolution and 16 days temporal resolution in their native projection. The downloaded data span the period from February 2000 until end of 2018 and cover the area between 10° E and 30° W longitude, 36.5° N and 71.5° N latitude, ~~that is represented by~~ corresponding to the spatial extent of the CORINE land cover information ~~of 2012~~ (see section 2.1.3) ~~and span the period from February 2000 until end of 2018~~.

Based on the pixel reliability information, we only retained records with good or marginal quality for subsequent analyses. Consequently, for most of the grid cells the VI time series contained missing values due to temporary clouds or snow cover. If the number of missing values was larger than the number of VI records, we considered the representing records as insufficient for our analyses and consequently removed the corresponding pixel from the analysis. However, since ~~high-elevation as well as high-latitude pixels had many missing values in winter and spring because of clouds and snow cover and we only were interested in VI during peak season~~we were only interested in VI time series during the growing season, we only considered the period from beginning of March (DOY 64) to end of October (DOY 304) for the definition of valid pixels. Following these selection criteria, we retained 95,523,236 pixels for the final analyses, representative of an area of 5,~~970,202~~097,215 km².

Prior to the analyses, VI time series of the retained pixels were further processed. We linearly interpolated the missing values of the corresponding VI time series for each pixel using the previous and succeeding records (Misra et al., 2016, 2018). To visualize the potential influence of this gap-filling procedure, we provide Fig. S1 which depicts the number of gaps filled in 2003 and 2018. Since more than 66% of the pixels rendered one or zero gaps, and 95 % rendered five or less gaps (i.e. less than one third of corresponding images missing, thus presumably sufficient data for meaningful interpolation) we assume any potential biases caused by the gap-filling procedure to be marginal. Subsequently, we removed negative outlier values from each VI time series by computing standardized residuals to a Gaussian-filtered (filter size of 80 days, i.e. 5 MODIS time steps), smoothed time-series. Residuals exceeding two negative standard deviations were replaced by the equivalent value of the smoothed time series (see also Misra et al., 2018, 2016). We smoothed the interpolated, outlier-corrected time series by reapplying the Gaussian filter. This procedure was necessary to efficiently handle the remaining high-frequency variability in the seasonal VI-cycle (Misra et al., 2016, 2018).

Finally, VI time series were detrended individually for each pixel ~~individually~~ by determining the linear trend of VI for each pixel and subtracting the pixel-specific trend from the corresponding pixel. This detrending was necessary to compensate

trends that were reported for vegetation indices (Bastos et al., 2017) which were also apparent in the downloaded data (Fig. S2~~1~~). A comparison between non-detrended and detrended data revealed similar spatial patterns with respect to between-pixel variability, however with amplified differences between 2003 and 2018 in the raw, non-detrended data. That is, for the raw data, the observed trend caused in dependence of its sign lower or higher peak-season VI values in 2003 compared to 2018, thereby introducing an offset between these two drought events. Concluding, the detrending was able to efficiently handle the varying VI-trends over the MODIS-era, while spatial patterns were generally retained.

Both NDVI and EVI are considered as proxy for photosynthetic carbon fixation, and thus allow for assessing possible changes in productivity in dependence of environmental conditions (Huete et al., 2006; Myneni et al., 1995; Xu et al., 2011). ~~Moreover,~~ NDVI has earlier been used in the context of drought monitoring (Anyamba and Tucker, 2012) and assessing impacts of drought on ecosystems on large scales (Orth et al., 2016; Xu et al., 2011). While NDVI relies on information derived from the red and near infrared spectra (see equation 1) EVI additionally makes use of the blue spectrum (see equation 2) to reduce atmospheric disturbance and influence of the understory:

$$NDVI = \frac{NIR - RED}{NIR + RED} \quad (1)$$

$$EVI = G \cdot \frac{NIR - RED}{NIR + C_1 \cdot RED - C_2 \cdot BLUE + L} \quad (2)$$

With G being the gain factor, C_1 and C_2 being the spectrum-specific coefficients of the aerosol resistance term, and L the canopy background adjustment term (G = 2.5, C_1 = 6, C_2 = 7.5, L = 1 for MODIS EVI, see Huete et al., 2002). Given these definitions, NDVI is more chlorophyll sensitive, while EVI is more sensitive to canopy structural variations (Huete et al., 2002). Thus, NDVI is more likely to reflect changes in leaf coloration as for instance in course of premature leaf senescence under drought, whereas EVI may better reflect early leaf shedding. For reasons of simplicity and to render our results comparable to previous studies which all used NDVI, we focus on results derived from NDVI. To provide the full picture, ~~which are generally confirmed by~~ results derived from EVI ~~as~~ are shown in the supplementary information generally confirming the results based on NDVI.

2.1.3 CORINE land cover information

To get an impression on the drought-impact on key European ecosystem components, analyses were stratified using the Coordinated Information on the European Environment land cover map (CORINE, https://land.copernicus.eu/pan-european/corine-land-cover~~/clc 2012~~) at ~~MODIS~~ 100 m resolution. Since land cover may change over time, we used two different time-steps of the Corine land-cover map, i.e. representative of 2000 and 2018. The land cover maps ~~was~~ were re-projected (as were the gridded climate data) to MODIS native projection and resolution using the nearest neighbour method,

thereby retaining the original land-cover classes. Given their dominance in Europe and their importance for land-use, we constrained this stratification to pastures, arable land, as well as coniferous, mixed, and broadleaved forests. Consequently, all pixels which either changed their land-cover from 2000 to 2018 and/or did not belong to the five selected land cover types were discarded from further analyses. Based on this selection procedure, we eventually retained 46,908,871 pixels, representative of an area of 2,503,104 km². Figure S3 depicts all pixels used for further analyses as well as their specific land cover class.

2.2 Statistical analyses

To quantify weather conditions for the years 2003 and 2018 in relation to average conditions, standardized anomalies of 500 hPa geopotential height, ~~heat load~~Tmax, and CWB were calculated. To account for seasonal-specific climate parameter distributions, standardization was performed month-wise, i.e. for instance for all CWB-January values. Before doing so, we tested the underlying assumption of normal distribution by computing Shapiro test for each grid cell and climate parameter respectively (Fig. ~~S2~~S4). The number of significant tests ($p < 0.001$) indicating non-normal distribution was in the order of expected false positives (0.0-0.~~3~~ 1 percent vs. 0.1 percent type I error probability). Therefore, we considered the assumption of normality to be fulfilled. To derive anomalies, we first computed the mean and standard deviation for all variables for the full period (1981-2018). Subsequently, we ~~for 2003 and 2018~~ determined the difference between 2003 and 2018 of the respective metric to its corresponding mean in units of standard deviations which in the following are called standardized anomalies (this procedure is also known as z-transformation). To assess the spatio-temporal development of Tmax and CWB for the two distinct drought events, we first of all mapped and evaluated integrated Tmax and CWB from January through October for 2003 and 2018 (see supplementary videos V1 and V2). Moreover, we also pooled Tmax and CWB anomalies for Northern Europe (north of 55°N latitude), Southern Europe (south of 45°N latitude), and Central Europe (in between) and compared the temporal development of mean anomalies between 2003 and 2018 for the three regions. Both Tmax and CWB indicated that the drought of 2003 peaked in August, whereas the drought of 2018 peaked in July. Consequently, to compare ecosystem response during the peak of drought we focused our comparison between 2003 and 2018 on these two time-steps, i.e. August 2003 vs. July 2018.

Thus, for integrated geopotential height, ~~heat load~~Tmax, and CWB we ~~obtained~~ eventually used each one standardized anomaly per grid cell for August 2003 and July 2018. The resulting standardized anomalies were mapped and statistically evaluated using histograms. Histograms were used to depict the absolute area representing climate anomalies in 2003 and 2018 which were compared among each other as well as to a normal distribution as a representation of conditions as expected in ~~normal~~ years representative of average conditions.

To quantify the response of European ecosystems to the two drought events, we focused on end-of-August (DOY 241) and end-of-July (DOY 209) VI values for 2003 and 2018, respectively. The selection of ~~this~~ these particular dates ~~represents a compromise between proximity to peak season (end of June, before maximum temperatures had been reached) and the occurrence of heat waves (end of July to mid of August)~~was based on the peak of climatological drought (see previous

paragraph). Since VI features a bounded distribution (values between -1 and +1), we could not apply a standardization approach as for the climate variables. Therefore, we computed for each VI time series its end-of-July quantiles over the 19 years similar to Orth et al. (2016). The corresponding quantiles were mapped for August 2003 and July 2018. Areas representing the 19 different quantiles were extracted and compared between August 2003 and July 2018 in a histogram. To depict the temporal development of drought responses in 2003 and 2018, corresponding VI quantiles of areas featuring a CWB anomaly lower than -2 were averaged for each time-step over a compromise of growing seasons, (i.e.(beginning on ~~January~~ May ~~1st~~9th until November 1st with 16 days interval) and visually compared to each other. To complement these analyses, we also mapped and evaluated VI quantiles from May 9th to November 1st for 2003 and 2018 in a similar manner as for Tmax and CWB (see supplementary videos V3 and V4). These spatiotemporal analyses generally confirmed the selection of August 2003 and July 2018 to represent the peak of drought impact on selected ecosystems.

Since we were aiming at a better understanding of particular ecosystems' response to drought severity, we subsequently pooled VI quantiles according to three classes of CWB anomalies (abnormal water deficit: CWB < -2, ~~average water~~weak water deficit ~~supply~~: -2 < CWB < ~~2~~0, ~~abnormal water surplus~~no water deficit: CWB >~~2~~0) and the chosen five CORINE land-cover classes (arable land, pastures, coniferous forest, mixed forest, broadleaved forest). For the resulting 15 combinations, we ~~again~~ compared the areas representing the 19 different quantiles between 2003 and 2018 as done for the total scene. Since the areas of CWB-land cover combinations differed between 2003 and 2018, we moreover computed histograms expressing proportional areas for 2003 and 2018. To get an impression on the absolute share of land cover types in regions that were defined as being under drought in August 2003 and July 2018 we provide Figure S5.

Finally, we aimed at developing empirical relationships between CWB anomalies and VI quantiles for the five CORINE land-cover classes mentioned before. For this, we logit transformed VI-quantiles (quantiles ranging from 0 to 1) to obtain an unbounded distribution and subsequently extracted the corresponding mean of transformed VI-quantiles for each CWB grid-cell (thus n = ~~2312~~2507). To assess the effect of different land cover classes, we extracted both the mean ~~E~~VI-quantiles representing all five land cover classes as well as for each land cover class separately. For the corresponding ~~2312~~ 2507 CWB-pixels we computed linear regressions between the transformed ~~E~~VI-quantiles as the dependent variable and CWB anomalies as independent variable separately for 2003 and 2018 and for the six different land cover types (i.e. five separate classes as well as their combination).

For linear regression evaluation, we report adjusted r^2 and display scatterplots of logit-transformed VI quantiles vs. CWB along with the corresponding regression line. Moreover, regression slopes were compared statistically for each land cover type between August 2003 and July 2018. For this, each slope estimate was bootstrapped using random subsampling over 1000 iterations and the overlap of 95 % confidence intervals was evaluated. That is, in case the confidence intervals of a respective comparison did not overlap, we considered the difference between slopes as significant. In a similar manner, we compared model slopes among ecosystems (i.e. pastures, arable land, as well as coniferous, mixed, and deciduous forest) separately for August 2003 and July 2018. Model slopes were grouped according to their overlap of 99.9 % confidence intervals. Finally, to backup observations made from our analyses we also computed a global model (n = ~~4624~~5042) by applying a linear mixed

effects model (lme) to ~~E~~VI quantiles using climatic water balance as fixed effect and incorporating crossed random slopes of land cover and year. All analyses were performed in 'R' (R core team, 2019) extended for the packages, 'nlme' (Pinheiro et al., 2017), 'raster' (Robert J. Hijmans, 2017), and 'SPEI' (Beguería and Vicente-Serrano, 2013).

3 Results

All considered climate parameters indicated abnormal weather conditions for July 2018 (Figs. 1-3). The integrated 500 hPa geopotential height, an indicator of the persistence of the atmospheric circulation, expressed anomalies in the order of two positive standard deviations for large parts of Central and Northern Europe, mainly covering the Baltic Sea region (Fig. 1 b). In comparison, July 2018 differed from August 2003 by featuring a dipole of 500 hPa geopotential height anomalies. While in August 2003 most of Europe featured ~~strong~~ positive anomalies, the Mediterranean was characterized by negative~~low~~ geopotential height anomalies in 2018 (Fig. 1 a vs. Fig. 1 b). The observed dipole of July 2018 expressed a bimodal distribution of anomalies, while August 2003 featured a skewed distribution towards positive anomalies (Fig. 1c). Consequently, in July 2018 the area featuring positive anomalies was 0.~~55~~61% of the area in August 2003, i.e. ~~3.1~~1.8 million km² vs. ~~5.7~~3.0 million km² ~~in 2003~~. At the same time, the area with negative anomalies was ~~3.7~~2.4 times higher in 2018, i.e. ~~3.5~~2.0 million km² in 2018 vs. ~~0.9~~0.8 million km² in 2003 (Fig. 1c).

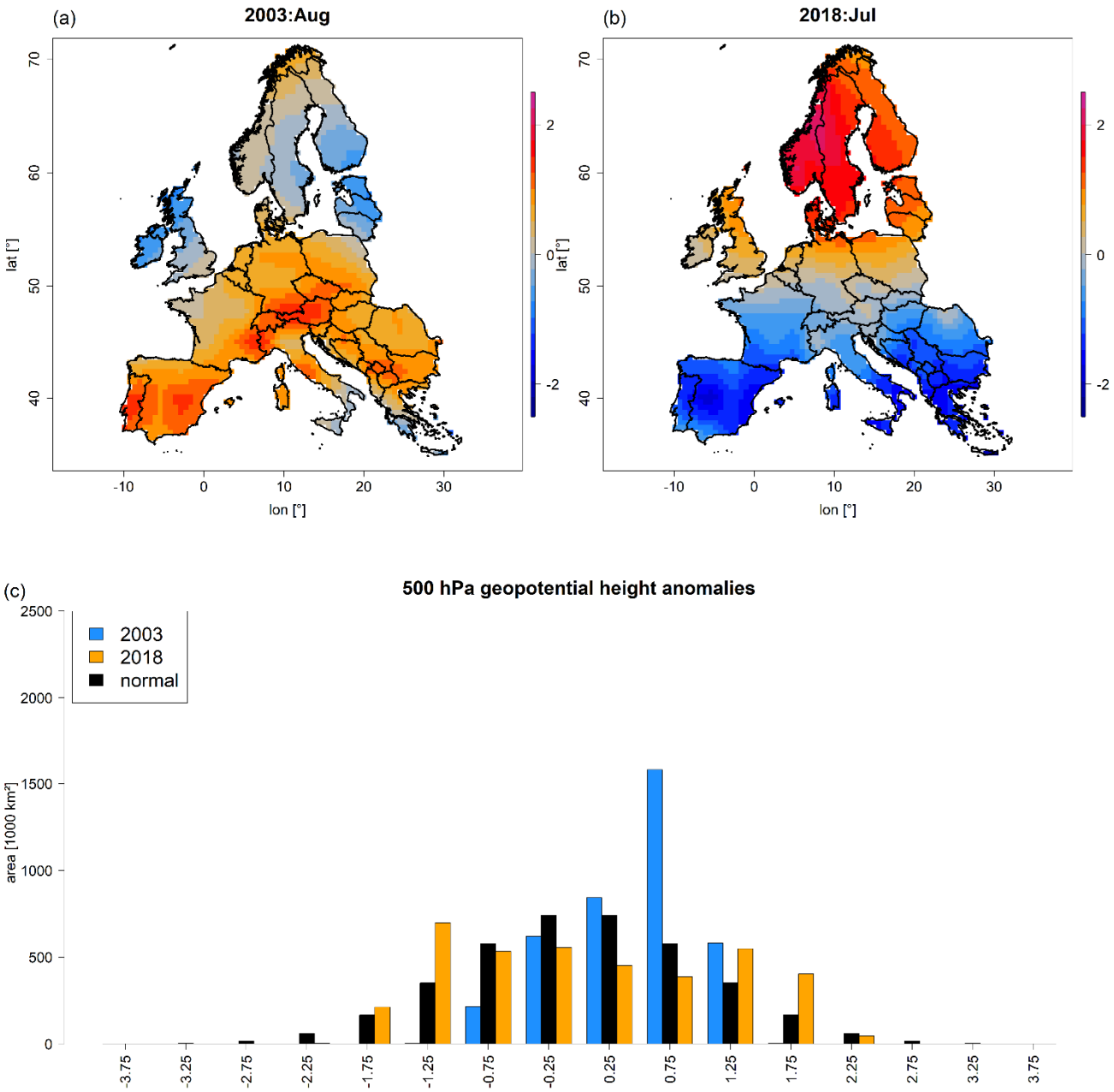

Figure 1: Maps depicting standardized anomalies of April-July 500 hPa geopotential height for 2003 and 2018 (a, b) as well as corresponding area histograms (in units of 1000 km²) for 2003 (blue), 2018 (orange), compared to a normal distribution (black) (c). Blue colours in (a) and (b) indicate geopotential height lower than average, whereas red colours indicate above average geopotential height in comparison to the 1981-2018 mean.

~~Heat load anomalies~~Anomalies of Tmax revealed up to four positive standard deviations (i.e. extreme heat) over large parts of Central and Northern Europe in 2018 (Fig. 2 b). In contrast, the Mediterranean featured average conditions (i.e. slightly warmer or cooler) and ~~strong~~ negative anomalies on the Iberian Peninsula. Although the total area with positive ~~heat load~~Tmax anomalies was more or less similar in August 2003 and July 2018 (Fig. ~~2b vs. 2a~~2c), anomalies above two positive standard deviations covered a ~~7.1~~1.9 times larger area in 2018, i.e. ~~3.3~~4.0 million km² vs. ~~0.5~~2.1 million km² in 2003 (Fig. 2c). Most contrasting differences between August 2003 and July 2018 were observed ~~in Southern Italy~~on the Iberian peninsula (hot in 2003, cool in 2018) as well as Scandinavia and the Baltic Sea region (~~cool~~ average in 2003, hot in 2018). The temporal assessment of Tmax anomalies revealed that particularly Northern Europe but also Central Europe experienced strong positive anomalies in 2018 that were higher compared to 2003 (Fig. S5). For Southern Europe the opposite was observed, i.e. less extreme Tmax anomalies in 2018 compared to 2003. Regarding the timing, the peak of the heatwave occurred one month earlier in 2018, i.e. July vs. August in 2003.

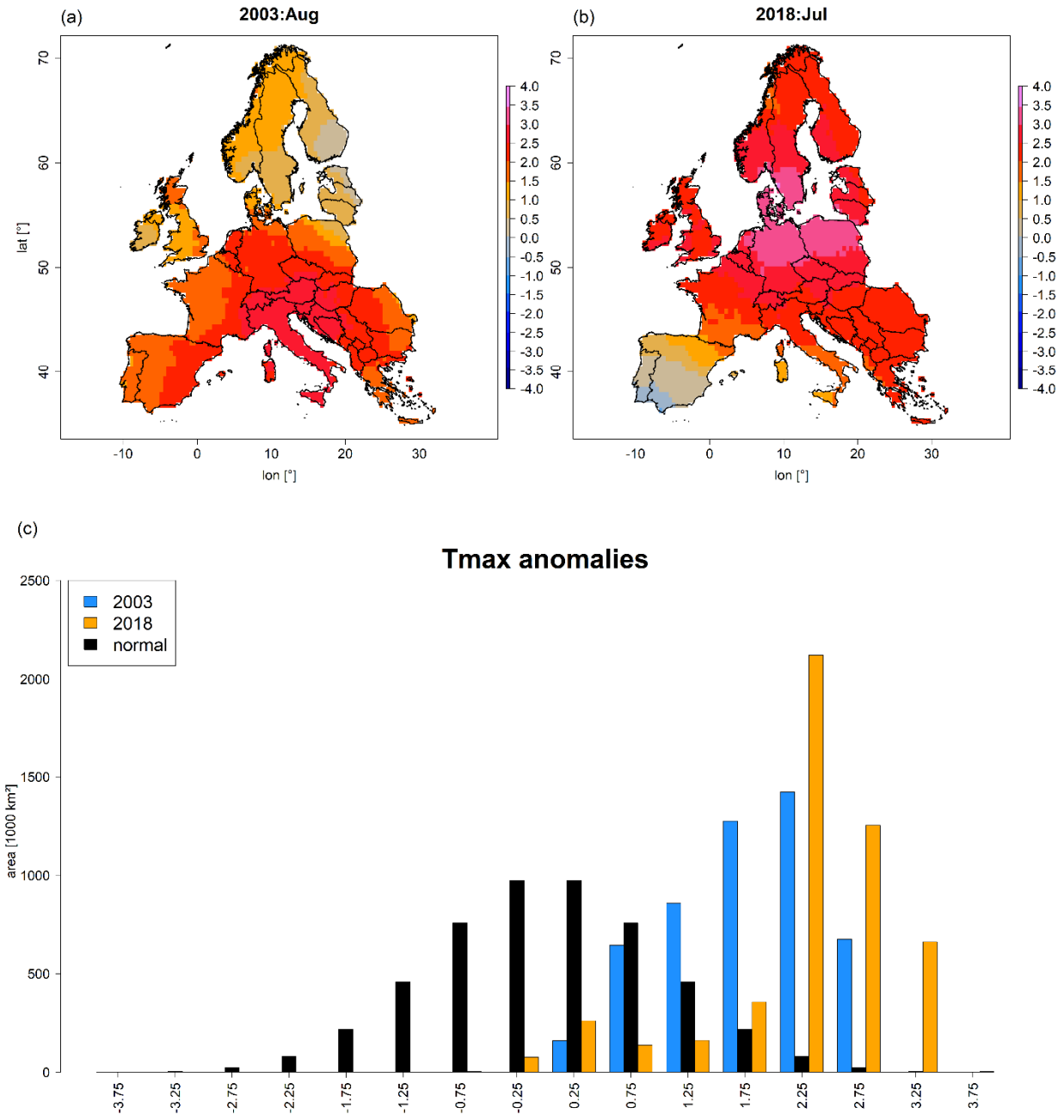

Figure 2: Maps depicting standardized anomalies of ~~April-July heat load~~Tmax for August 2003 and July 2018 (a, b) as well as corresponding area histograms (in units of 1000 km²) for 2003 (blue) and~~,~~ 2018 (orange), compared to a normal distribution (black) (c). Blue colours in (a) and (b) indicate relatively cool conditions, whereas red colours indicate warmer conditions in comparison to the 1981-2018 mean. Time-series depicting the temporal development of Tmax anomalies for Northern, Central, and Southern Europe are shown in supplementary Fig. S5. A video depicting the spatio-temporal development of Tmax anomalies from January through October is provided in supplementary V1.

For 2018, CWB ~~for 2018~~ revealed patterns largely consistent with ~~heat load~~Tmax (Fig. 3b). Again, Central and Northern Europe featured extreme negative (thus dry) deviations, while the Mediterranean generally expressed positive (thus moist) deviations. In comparison (Fig. 3b vs. 3a), the area with negative (i.e. dry) CWB anomalies was ~~relatively similar in both years~~slightly higher in 2003, i.e. 4.2 million km² in August 2003 vs. 3.9 million km² in July 2018 (Fig. 3c). However, if considering CWB anomalies below two negative standard deviations (i.e. extreme drought), in July 2018 an area ~~5~~1.~~3~~ 4 times larger than in August 2003 was affected, i.e. 1.~~7~~ 1 million km² ~~in 2018 in~~ vs. ~~0.3~~0.8 million km² ~~in 2003~~ (Fig. 3c). Consequently, the contribution of the five land cover types under consideration featuring CWB anomalies below two negative standard deviations, revealed a 1.3 times higher overall spatial contribution in July 2018 compared to August 2003, i.e. 610,000 km² vs. 460,000 km² (Fig. S6). These differences were mostly related to coniferous forests due to the more northern location of the drought 2018.

Regarding the spatiotemporal assessment of CWB anomalies, 2003 and 2018 featured a contrasting development (Fig. S5 and supplementary video V2). While Northern Europe experienced strong water deficit from May through August in 2018 and more or less normal conditions in 2003, Southern Europe was characterized by pronounced water deficit from June to September 2003 while it showed positive anomalies throughout the whole growing season in 2018. Central Europe, however expressed more or less comparable conditions at the peak of drought (August 2003 vs. July 2018), but here, drought conditions began earlier in 2003 compared to 2018. Concluding the climatological assessment of the two drought events, 2003 featured a later peak of drought (August) and was centred around Southern and Central Europe while 2018 featured an earlier peak of drought (July) that was centred around Central and Northern Europe.

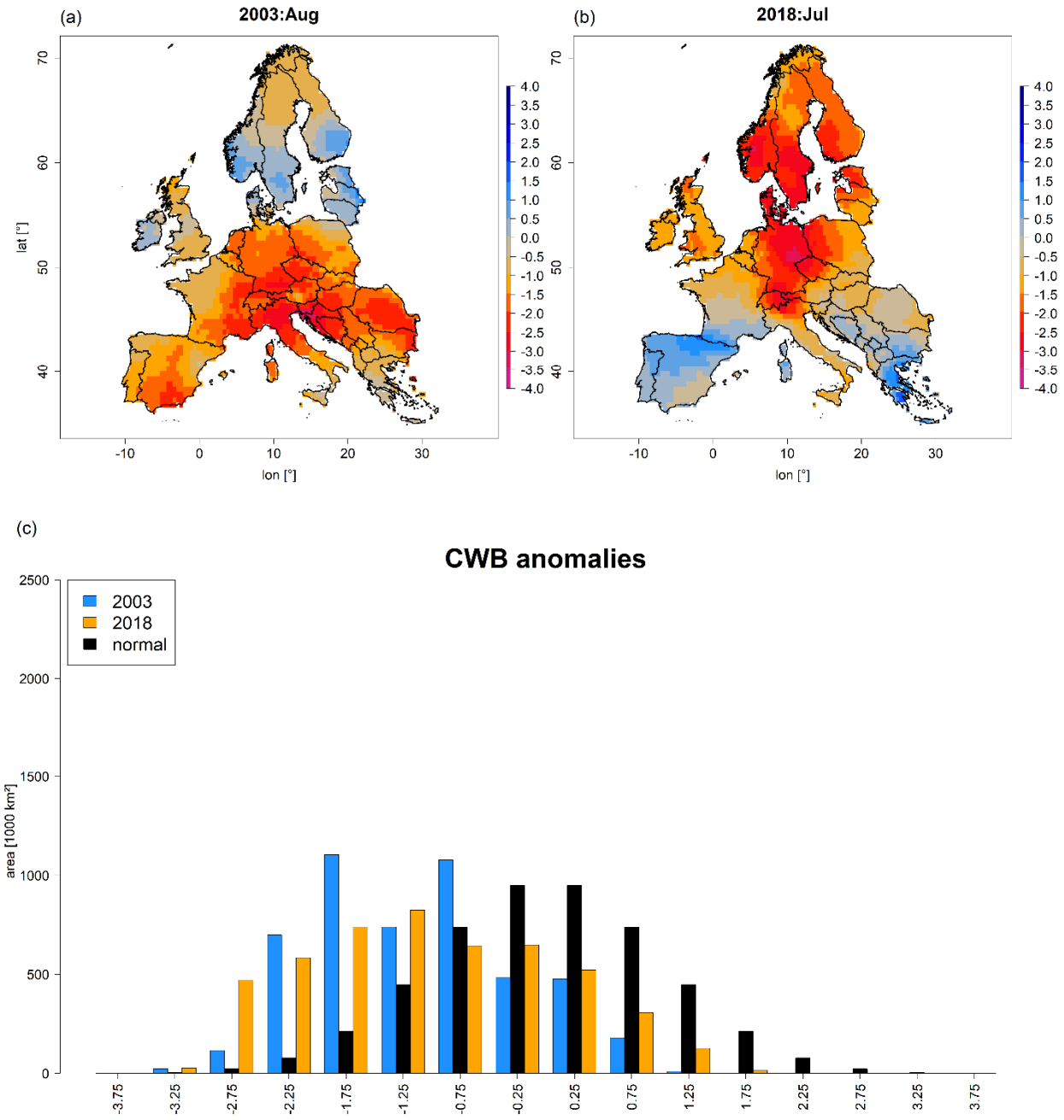

Figure 3: Maps depicting standardized anomalies of April-July climatic water balance for 2003 and 2018 (a, b) as well as corresponding area histograms (in units of 1000 km²) for 2003 (blue), 2018 (orange), compared to a normal distribution (black) (c). Blue colours in (a) and (b) indicate relatively moist conditions, whereas red colours indicate dryer conditions in comparison to the 1981-2018 mean. Time-series depicting the temporal development of CWB anomalies for Northern, Central, and Southern Europe are shown in supplementary Fig. S5. A video depicting the spatio-temporal development of CWB anomalies from January through October is provided in supplementary V2.

~~End of July v~~Vegetation response – as approximated using satellite-based vegetation indices – indicated ~~-~~clear differences between August 2003 and July 2018. We found low NDVI quantiles in large parts of Central Europe, Southern Scandinavia, and the Baltic Sea region and high quantiles in the Mediterranean in July 2018 (Fig. 4b). In ~~comparison~~contrast, 2003 featured low NDVI quantiles in Western, Central, and Southeast Europe and high quantiles in Northern Europe (Fig. 4a). The most prominent difference between July 2018 and August 2003 was the ~~2-~~1.5 times larger area featuring the lowest quantile, i.e. ~~822,067~~409,000 km² in July 2018 vs. ~~408,614~~272,000 km² in August 2003 (Fig. 4c). At the same time, a ~~2-~~1.7 times larger area featured the highest quantile in July 2018, i.e. ~~439,460~~117,000 km² vs. ~~214,922~~68,000 km² August in 2003 (Fig. 4c). According to NDVI quantiles, hotspots of drought-response in July 2018 were located in Ireland, United Kingdom, France, Belgium, Luxemburg, the Netherlands, Northern Switzerland, Germany, Denmark, Sweden, Southern Norway, Czech Republic, Poland, Lithuania, Latvia, Estonia, and Fin~~n~~land.

Figure 4: MODIS NDVI quantiles representing peak~~-~~ ~~of season~~ ~~drought~~ conditions at the end of ~~July~~ August (DOY ~~209~~241) in 2003 (a) and end of July (DOY 209) in 2018 (b) for the five selected land-cover types as well as the corresponding area histograms (in units of 1000 km²) representing the nineteen NDVI quantiles (c). Blue colours in (a) and (b) indicate upper quantiles (thus a higher than average vegetation greenness), while orange to red colours indicate lower anomalies (i.e. lower than average vegetation greenness). Blue bars in (c) refer to 2003 and orange bars to 2018. Complementary results for MODIS EVI are shown in supplementary Fig. ~~S4~~S7. Videos depicting the spatio-temporal development of NDVI and EVI are shown in supplementary V3 and V4.

In regions with water deficit (CWB anomalies below - 2 SD and below 0 SD; Figs. ~~5c~~5a, 5b, respectively) we found a higher frequency of low NDVI quantiles compared to upper quantiles. In detail, regions with extreme water deficit (5a), featured higher absolute areas with low NDVI quantiles for all land cover classes but broadleaved forest in 2018 compared to 2003. In regions with weak water deficit (5b), absolute areas were more similar between 2003 and 2018 but coniferous and mixed forests featured larger areas with low quantiles in 2018. Similarly, regions with ~~water surplus~~no water deficit (CWB anomalies above ~~> 2~~ 0~~SD~~; Fig. ~~5a~~5c) featured higher frequencies ~~for~~ of upper quantiles compared to lower quantiles which however was more pronounced in 2018 ~~compared to 2003~~for pastures, arable land, and broadleaved forests and more pronounced in 2003 for coniferous and mixed forests. ~~Interestingly, normal conditions (Fig. 5b) featured an inconsistent picture for the different land-cover classes in both years.~~ The most prominent difference was related to absolutely larger areas being affected by water deficit ~~and surplus~~ in 2018 compared to 2003 (see also Fig. S6), particularly considering lowest VI quantiles for coniferous forests with a more than 8 times higher area in 2018 (Fig. 5a). If considering relative frequencies, histograms of 2018 and 2003 became more similar but yet revealed a higher proportion of ~~negatively affected coniferous and mixed forests~~lowest quantiles in 2018 (Fig. ~~S3~~S8).

The temporal development of NDVI quantiles from the corresponding drought regions (CWB anomaly < -2 in August 2003 vs. July 2018) ~~was rather similar~~differed between ~~2018 and 2003~~the two events (Fig. 6). While pastures featured rather similar

temporal patterns of NDVI quantiles in the two years, arable land as well as the three considered forest types featured lower mean quantiles over most of the growing season and particularly in early summer. ~~On average~~In combination, the 2018 time series featured lowest mean quantiles ~~around DOY 209~~at the end of July, while the 2003 lowest mean quantiles occurred during August. ~~Most prominent differences between the two events were observed for coniferous and mixed forests, which revealed lower mean quantiles in 2018 while the negative peak of quantiles appeared to occur later for pastures and arable land in 2003.~~

The impression of CWB affecting NDVI quantiles was underpinned by the linear regressions between the logit-transformed NDVI quantiles and the CWB-anomaly in 2003 and 2018, respectively (Fig. 7a-f). For all land-cover classes a significant and positive effect of climatic water balance on NDVI quantiles was observed, particularly in 2018. Explained variance (r^2) and bootstrapped model slopes were consistently higher in 2018 compared to 2003 (Fig. 7g). In addition, r^2 and model slopes were highest for pastures in both years ~~highest for pastures~~, followed by arable land, and the three forest types which did not differ among each other in 2018 while broadleaved and mixed forests featured smaller slopes compared to coniferous forests in 2003 (lower case letters in Fig. 7g). The linear mixed effects model over all land-cover classes and the two years confirmed the significant fixed effect of climatic water balance on logit-transformed NDVI quantiles (marginal r^2 = 0.~~47~~37). Incorporation of random slopes related to land cover and year increased explained variance by ~~9~~ 33 percent (conditional r^2 = 0.~~51~~48), confirming the varying effect of the two drought events as well as the differing impact on different land-cover classes. All presented results based on NDVI are generally confirmed by complementary analyses using EVI (supplementary Figs. S7 and S~~4~~9-~~S7~~S12).

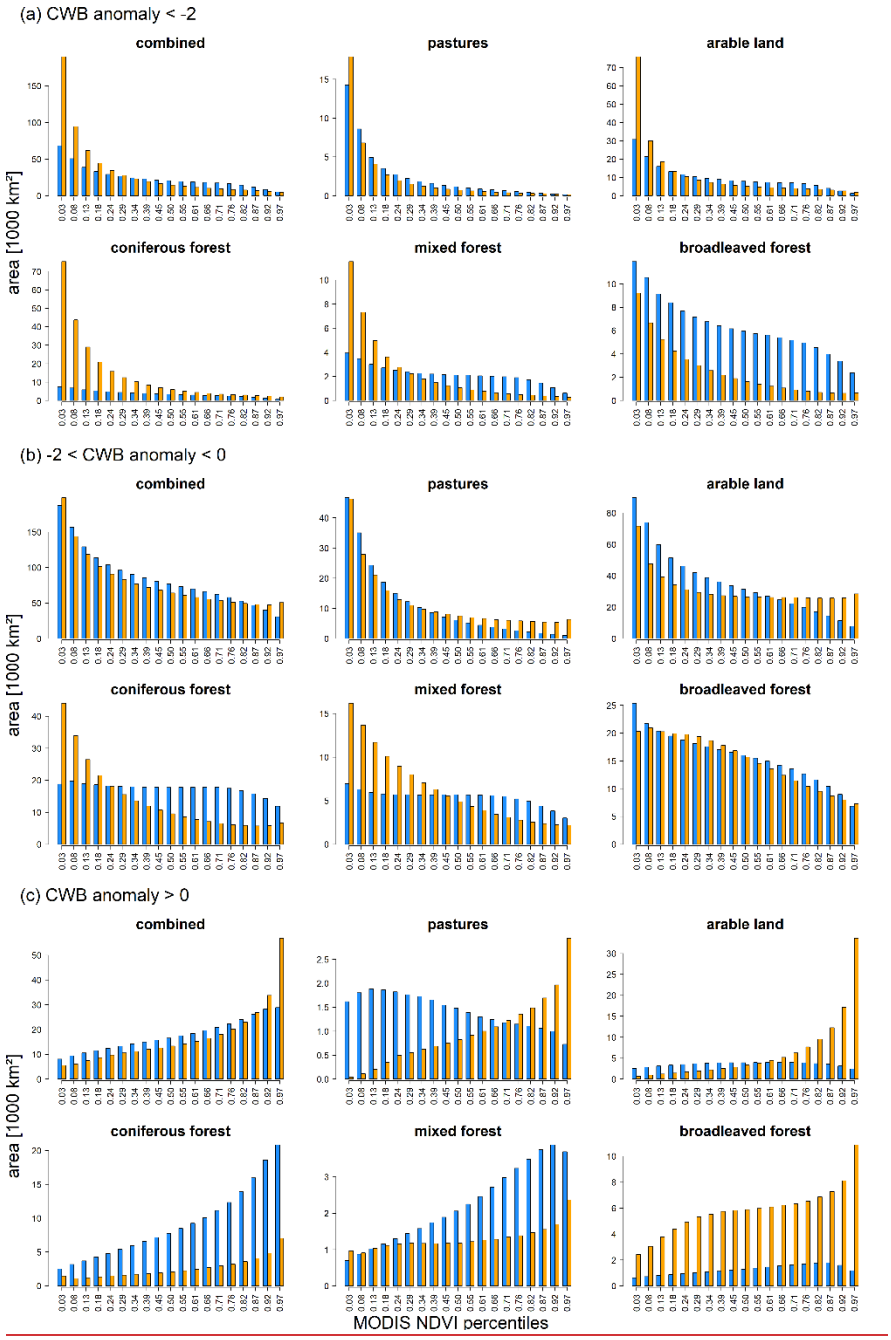

Figure 5: Histograms depicting the absolute areas (in units of 1000 km²) representing the nineteen NDVI quantiles pooled according to CORINE land-cover classes for regions ~~that featured~~with (a) extreme water ~~surplus~~ deficit (CWB-anomaly ~~>~~< -2) vs.~~,~~ (b) ~~average conditions~~weak water deficit (- 2 < CWB-anomaly < 0)~~,~~ and (c) no water deficit (CWB-anomaly ~~< 2~~> 0). Blue bars refer to 2003, orange bars to 2018. Histograms depicting the proportional areas are shown in supplementary Fig. ~~S3~~S8, results for MODIS EVI in supplementary Figs. ~~S5~~ S9 and ~~S6~~S10.

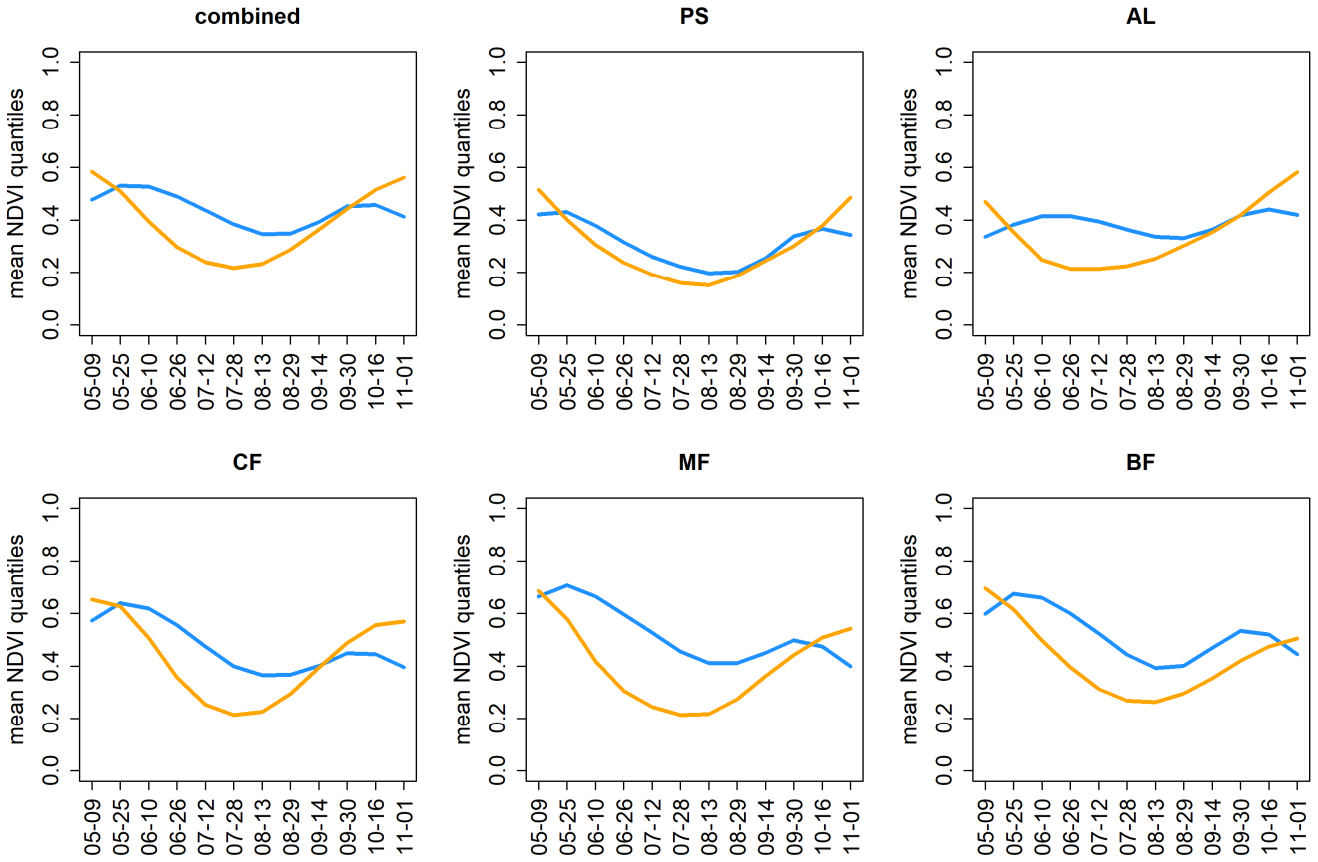

Figure 6: Time-series of NDVI-quantiles averaged over the regions featuring CWB < -2 ~~for~~ in August 2003 (blue) and July 2018 (orange) for the five different land-cover classes (b-f) and a combination of those (a). PS = pastures, AL = arable land, CF = coniferous forest, MF = mixed forest, BF = broadleaved forest. Complementary results for MODIS EVI are shown in supplementary Fig. S11.

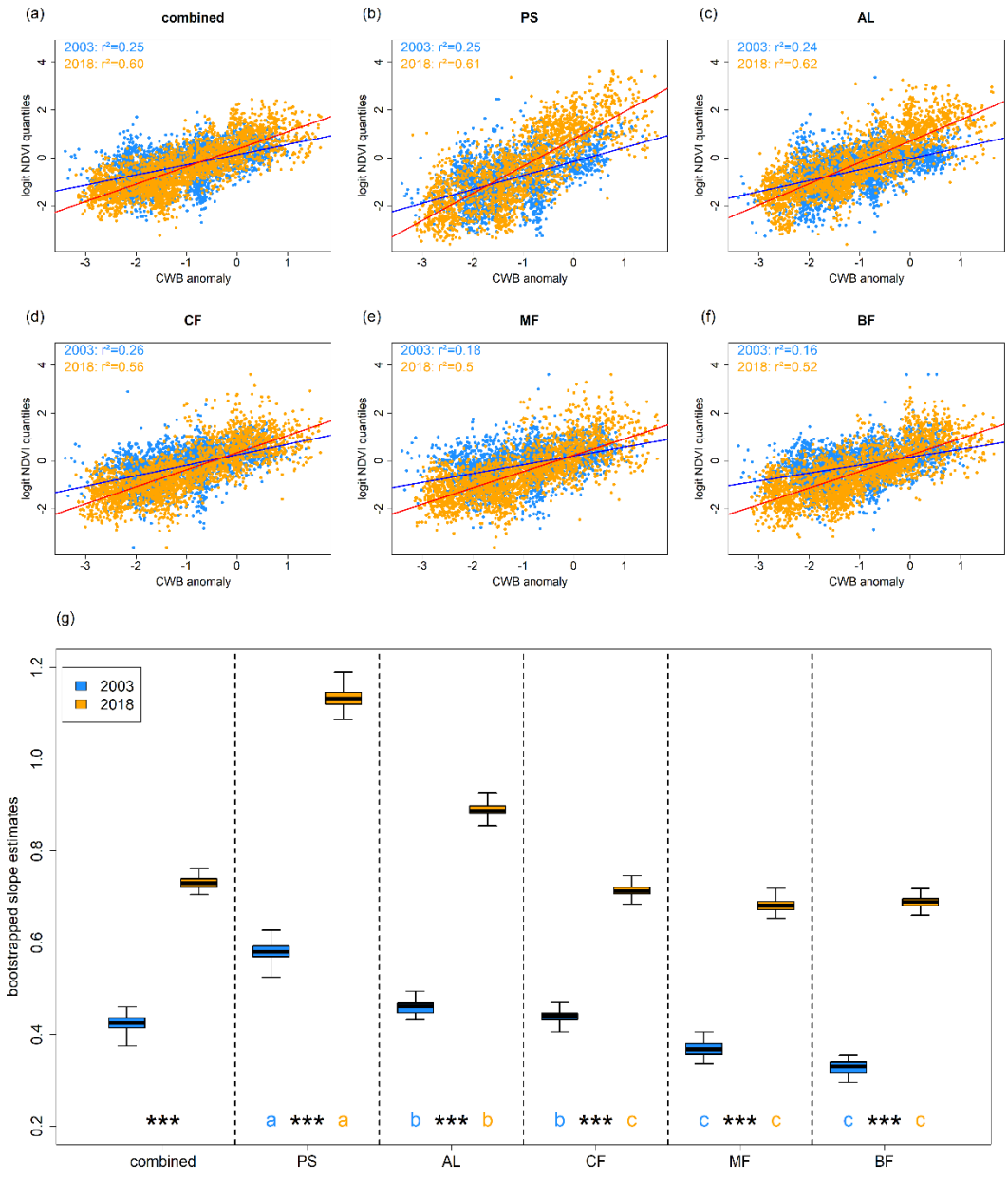

Figure 7: (a-f) Scatterplots depicting the relationship between average logit-transformed NDVI-quantiles and mean CWB of the 100 CWB percentiles in 2003 (blue) and 2018 (orange) for pastures (b), arable land (c), coniferous forests (d), mixed forest (e), broadleaved forest (f) and a combination of those (a). Blue lines depict the regression line for 2003, red lines for 2018. (g) Bootstrapped regression slope estimates for the five different land-cover classes as well as their combination. Minor case letters refer to group assignment of land-cover classes according to the overlap of 99.9 % confidence intervals of bootstrapped slopes in 2003 (blue) and 2018 (orange). Significance stars (***) indicate no overlap between 99.9 % confidence intervals of 2003 and 2018 for the respective land-cover class. PS = pastures, AL = arable land, CF = coniferous forest, MF = mixed forest, BF = broadleaved forest. Complementary results for MODIS EVI are shown in supplementary Fig. ~~S7~~S12.

4 Discussion

4.1 Climatic framework

Based on the parameters considered for the quantification of summer conditions, 2018 clearly supersedes the record drought of 2003 (Figs. 1-3). The more ~~persistent~~ extreme anticyclonic circulation patterns for 2018 across Northern Europe as indicated by 500 hPa geopotential height likely triggered ~~the~~ stronger positive ~~heat load~~Tmax anomalies and more negative climatic water balance anomalies across Central and Northern Europe in comparison to 2003. Moreover, the two drought events differed regarding their timing and location, with 2018 featuring an earlier peak of drought (July vs. August in 2003) and a more northward centre around the Baltic Sea vs. the Mediterranean in 2003.

Anticyclonic blocking situations – as indicated by strong positive 500 hPa geopotential height anomalies – have been reported at an increasing frequency in course of the satellite era (Horton et al., 2015) which likely relates to the increasing persistence of heatwaves observed over the past 60 years (Pfleiderer and Coumou, 2018) and the increasing frequency of a hemisphere-wide wavenumber 7 circulation pattern (Kornhuber et al., 2019). The resulting heatwaves are additionally enhanced by global warming and positive land surface – atmosphere feedback loops via soil moisture depletion and subsequent lack of latent cooling (Fischer et al., 2007). Moreover, summer temperatures and precipitation were reported to correlate negatively at mid latitudes which may amplify further according to CMIP5 climate projections (Zscheischler and Seneviratne, 2017). This renders the evaluation of ecosystem responses to compound events a key topic for climate change research (Zscheischler et al., 2018). Concluding, the prevailing extreme climatic conditions qualify 2018 as a key event for studying ecosystem-responses to hotter droughts in Europe.

4.2 Ecosystem impact

4.2.1 Stronger ecosystem impact in 2018

~~End of July~~The comparison of MODIS NDVI anomalies generally supported the impression of a more extreme drought in July 2018 compared to August 2003. Our analyses based on EVI generally confirmed this impression (Figs. S7 and S9-S12). That is, the area featuring the lowest quantile in July 2018 was ~~twice~~ 1.5 times as high compared to August 2003 (Fig. 4c). In accordance with the more northward location of the anticyclone, hotspots of negative ecosystem impact were concentrated in Central and Northern Europe in 2018.

In general, the spatial distribution of NDVI quantiles ~~matches~~ matched the observed climatic dipole of 2018 very well. Moreover, the bimodal response of European ecosystems is well in line with a report on European maize yield in 2018, with an observed strong increase (10% more than average) for e.g. Romania and Hungary, a strong decrease (10% less than average) for e.g., Germany and Belgium, and the European level net effect estimated at a decrease in maize yield of around 6% (see public references: European Commission).

The bimodal behaviour and larger extent of ecosystem impact in 2018 was also reflected in land-cover specific area distributions of NDVI quantiles (Figs. 5a ~~and 5c~~and S6). That is, the area featuring lowest ~~(highest)~~ quantiles in regions with

extreme water deficit ~~(surplus)~~ was much larger in July 2018 compared to August 2003. Given the skewed distribution of VI quantiles in those regions, i.e. more lower quantiles in regions with ~~strong~~ extreme negative CWB anomalies and more upper VI quantiles in regions with ~~strong~~ positive CWB anomalies, the response of these ecosystems appears to be governed by prevailing climate conditions, in particular climatic water balance.

This impression was underlined by linear regressions, which revealed a strong and significant positive impact of CWB on NDVI quantiles in both years and for all land-cover types (Figs. 7a-f). It is noteworthy, that 2018 was characterized by a higher explained variance and significantly more positive model slopes in comparison to 2003 (Fig. 7g). These impressions from single linear models were generally supported by the linear mixed effects model, which showed an increase of r^2 at about ~~9~~ 35 percent when incorporating land-cover and year as random effects.

We want to note that we also observed small areas (ca. 1000 km² for each of the considered land cover classes) of high quantiles in regions featuring extreme drought. This observation is likely related to the different resolution of climate data (0.5°, thus ca. 50 km x 50 km) vs. MODIS (231 m x 231 m). Using such relatively coarse climate data for quantifying drought neglects elevation-driven climatic variations within grid cells (Zang et al., 2019) in contrast to the relatively higher resolution of MODIS which likely captures such differences. For instance, mountain ranges – which on average feature cooler temperatures (thus less evapotranspiration) and higher precipitation – likely feature less extreme water deficit compared to surrounding lowlands which may cause higher VI values than one would expect if only considering the drought classification of the corresponding climate grid cell. In addition, groundwater availability – which may vary within climate grid cells, particularly in proximity to rivers and lakes – may locally modulate plant water availability, possibly explaining some of the observations of high VI quantiles under extreme drought.

Furthermore, quantifying drought on anomalies alone bears the risk to erroneously classify regions that actually feature water surplus (CWB > 0) as being drought-affected (Zang et al., 2019). This is likely to happen in regions which usually have high water surplus (e.g. the Norwegian west-coast) and thus may feature more than two negative CWB standard deviations even though raw CWB is positive (Zang et al., 2019). For both 2003 and 2018, 5 (1) percent of climate grid cells featured positive CWB even though CWB anomalies indicated (extreme) water deficit (CWB < 0 and CWB < -2 SD, see also Fig. S13). This false classification may explain some of the observed highest quantiles in regions that were classified as featuring extreme water deficit. Lacking a more advanced drought-metric that compensates for such effects, we followed the widely accepted approach to use standardized CWB for our analyses. To show the full picture, we point out potential biases caused by this approach (Fig. S13) as proposed by Zang et al. (2019). Given the relatively low number of potentially misleading extreme drought classifications (1 percent for each year) we estimate the impact on our analyses to be generally low.

Finally, we want to stress that the choice of VI used for quantification of the ecosystem response to drought matters. While Li et al. (2010) found stronger relationships and lower errors between NDVI and ground observations made in grasslands, shrublands and forest in comparison to EVI, Vicca et al. (2016) reported EVI to be more sensitive to reductions in GPP that were not reflected by leaf coloration or early leaf senescence. Therefore, we present results from both VIs which generally support each other (e.g. comparison between Figs. 4 and S7, Figs. 7 and S12) but focused on NDVI to make our contribution

directly comparable to previous studies dealing with drought impacts on ecosystems (Anyamba and Tucker, 2012; Orth et al., 2016; Xu et al., 2011). To complement our VI-based assessment, future studies may consider the use of solar-induced fluorescence which is known to be more sensitive to terrestrial photosynthesis (Li et al., 2018).

4.2.2 Location and timing of drought possibly drives stronger ecosystem response in 2018

The stronger coupling (higher r^2) between CWB and VI quantiles in July 2018 may be related to the period used to integrate CWB (~~April-July~~4 months), namely if the VI response of August 2003 were triggered by climatic anomalies over longer or shorter periods. To test this, we assessed the relationship of VI quantiles with CWB integrated over various ~~different~~ periods (e.g. including previous winter in CWB or shortening the period) which all revealed similar patterns, i.e. a stronger response to CWB in 2018 (not shown).

However, it seems possible that the stronger coupling of VI quantiles to CWB in 2018 is related to the earlier timing and more northward location~~spatial distribution~~ of drought and thus ~~the~~ different ecosystems being affected at an earlier stage of their seasonal cycle. In 2003, the ~~epicenter~~ centre of ~~the~~ drought was ~~located in Central France and~~in Central and Southern Europe ~~the Mediterranean~~ and peaked in August, i.e. it affected regions which host ecosystems that are ~~regularly~~ frequently experiencing summer drought at that time of the year and thus are likely better adapted to cope with dry conditions. In contrast, the circulation patterns of 2018 resulted in a drought-~~epicenter~~ centre in Central and Northern Europe earlier in summer, ~~Southern Scandinavia, and around the Baltic Sea~~, i.e. in regions with ecosystems ~~which~~ that are less adapted to extremely dry climatic conditions ~~such as in 2018~~ and therefore likely react strongly. The earlier timing possibly also triggered a stronger response to the drought in 2018, particularly in Northern Europe where it began as early as May, i.e. at the beginning of the growing season (Fig. S5 and V2). Northern European forests are dominated by coniferous forests that to a large degree consist of Norway spruce and Scots pine, i.e. two tree species that have been frequently reported to suffer under drought (e.g. Buras et al., 2018; Kohler et al., 2010; Rehschuh et al., 2017; Rigling et al., 2013). Moreover, coniferous forests provided a high share of the drought affected ecosystems in 2018 (Fig. S6). In combination, the potentially stronger reaction of high latitude coniferous forests may partly explain the observed stronger coupling between CWB anomalies and VI quantiles in 2018 compared to 2003. ~~-~~In addition, v~~V~~arious reports from dried-out pastures and cornfields as well as deciduous trees shedding their leaves in July and August in 2018 likely explain the record-low VI values for corresponding Central European ecosystems (see public news references and Fig. S14 for an example of early leaf senescence of European beech in 2018). At the same time, the usually summer-dry Mediterranean experienced water surplus, relaxing the general limitation of the associated ecosystems by plant water availability and leading to a generally higher greenness of the vegetation. Considering forest ecosystems, this interpretation is in line with Klein (2014), who reported higher leaf gas exchange and thus photosynthetic capacity under dry conditions in Mediterranean forests compared to temperate forests.

Nevertheless, our ~~hypothesis~~ hypotheses explaining the stronger coupling of VI quantiles with CWB in 2018 need~~s~~ further ~~investigation~~support, e.g. by studying the sensitivity and coupling of plant productivity with climatic properties for the considered land-cover classes as for instance done by (Anderegg et al., 2018). A sub-classification of land-cover classes seems

to be reasonable for such an analysis, in order to account for possibly differing drought-sensitivities of ecosystems represented by one specific land-cover class. For instance, Mediterranean coniferous forests comprise different species and are thus likely better adapted to drought than boreal coniferous forests in Scandinavia.

4.2.3 Forests featured a weaker immediate response to drought

In addition to the differences between the two drought events, we also observed differing sensitivities of VI quantiles to CWB among ecosystems, which were consistent over the two drought events. We found the highest regression slope estimates for pastures followed by arable land and forests (Fig. 7g). This likely reflects the higher climatic buffering function of forests in comparison to arable land and pastures. In forests, the micro-climate is generally less extreme, leading to lower ambient air temperatures and consequently a lower evapotranspiration in comparison to open fields (Chen et al., 1993, 1999; Young and Mitchell, 1994). Consequently, water resources are consumed more sustainably by forests. Moreover, if not growing on water-logged soils trees typically feature higher rooting depths compared to grasses and crops and therefore have access to deeper soil water reservoirs. Regarding the European drought of 2003, an accelerated soil moisture depletion of grasslands in comparison to forests has been reported earlier (Teuling et al., 2010). Also Wolf et al. (2013) found contrasting responses of grasslands vs. forests regarding water and carbon fluxes during a drought event in 2011. They observed an immediate negative drought-impact on the productivity of managed grasslands while mixed and coniferous forests simply reduced transpiration and maintained GPP, thereby increasing their water-use efficiency and decreasing soil-water consumption (Wolf et al., 2013).

4.2.4 Forest legacy effects

Nevertheless, European forests were in parts heavily affected by the drought 2018, as indicated by the distribution of VI quantiles (Fig. ~~5c~~5a). For instance, ~~140~~180,000 km² of drought affected (CWB < 0) coniferous forests featured the lowest quantile in 2018. Moreover, 45,000 km² of deciduous trees featured the lowest VI quantile in 2018 which likely relates to the observed early leaf-shedding of deciduous trees in Central Europe (see Fig. S14). First estimates ~~for North Rhine-Westphalia (Northwest-Germany) assume forest productivity losses of around 40% (see public references: Wald und Holz NRW)~~by German forestry about the total loss of wood volume as a consequence of the drought 2018 and the ongoing drought in 2019 were in the order of 105 million solid cubic meters (see public references, BMEL). ~~Moreover, 20,000 km² of deciduous trees featured the lowest quantile in 2018 which likely relates to the observed early leaf-shedding of deciduous trees in Central Europe (see public-news references).~~ Besides these direct impacts, carry-over effects are likely to be experienced in the following years: Evidence for delayed responses comes from remotely sensed vegetation activity in the aftermath of the 2003 event (Reichstein et al., 2007) and reports on observed die-back of Norway spruce, Scots pine, and European beech in spring and summer 2019 (GfÖ-workshop on drought 2018 held on June 4th, 2019 in Basel, see also public news references). These effects could partly be due to legacy effects in tree response to drought (Anderegg et al., 2015; Kannenberg et al., 2018) as well as tree mortality often occurring years after the event (Bigler et al., 2006; Cailleret et al., 2017). Support for an expected

delayed response of forests also comes from a severe drought in Franconia, Germany, in 2015, which resulted in increased Scots pine mortality, that was not recognized earlier than in the subsequent winter 2015/2016 and became even more pronounced in spring 2016 (Buras et al., 2018). From this event, we also learned that particularly forest edges – which feature an intermediate micro-climate between the forest interior and open fields – are more susceptible to drought-induced mortality (Buras et al., 2018). However, given the spatial resolution of the applied remote sensing products (231 m x 231 m), patches with tree dieback as well as forest edges could not be resolved, which should therefore be given attention in future studies.

4.3 Call for a European forest monitoring

Given likely legacy effects, studying the development of Central and Northern European forest ecosystems over the next years is particularly interesting and may reveal negative mid- to long-term responses as well as an increased tree mortality. In this context, we propose an ~~immediate~~ observation of forests within the outlined hotspots by combining satellite-based and close-range remote sensing techniques with dendroecological investigations and an eco-physiological monitoring (Buras et al., 2018; Ježík et al., 2015). ~~A timely~~The initiation of such monitoring campaigns would provide the unique opportunity to study natural tree die-back in real-time, thereby increasing our knowledge about drought-induced tree mortality (Cailleret et al., 2017). The recently released European forest condition monitor (~~http://www.lsai.wzw.tum.de/index.php?id=71&L=1~~www.waldzustandsmonitor.de) may be considered a first step towards a satellite-based, near real-time monitoring of European forests.

5. Conclusions

Based on climatic evidence, 2018 may be considered the new reference year for hotter droughts in Europe. However, the observed contrasting spatiotemporal patterns of the drought events in 2003 and 2018 highlight the complexity of ecosystem responses to severe droughts. More specifically, we observed a different sensitivity of ecosystems to CWB between the two events and a differing sensitivity of land cover classes to drought, with pastures and agricultural fields expressing a higher sensitivity in comparison to forests. The observed climatic heterogeneity and resulting ecosystem response poses certain challenges for estimating the effects on the carbon cycle in European ecosystems in 2018. That is, the observed dipole in 2018 makes it difficult to directly compare the European carbon budget of 2018 with 2003. Finally, legacy effects of forest ecosystems are likely to occur in course of the next years. Consequently, to obtain a more complete picture about the impact of the drought 2018 we recommend continued satellite-based remote sensing surveys to be accompanied by immediate in-situ monitoring campaigns. In this context, particular attention should be given to the outlined hotspots of the drought 2018, i.e. Ireland, United Kingdom, France, Belgium, Luxemburg, the Netherlands, Northern Switzerland, Germany, Denmark, Sweden, Southern Norway, Czech Republic, Poland, Lithuania, Latvia, Estonia, and Finnland.

Data Availability

The datasets analysed for this study are publicly available. Public web-links as well as the post-processing of data is described in the material and methods section of this article, wherefore all results are reproducible.

Author Contributions

AB and CSZ developed the study design. AB conducted all data processing and statistical analyses. Interpretation and refinement of statistical results was discussed among AB, AR, and CSZ. AB drafted the first version of the article which was further refined by AR and CSZ.

Competing Interests

The authors declare that the research was conducted in the absence of any commercial or financial relationships that could be construed as a potential conflict of interest.

Acknowledgements

This project is funded by the Bavarian Ministry of Science and the Arts in the context of the Bavarian Climate Research Network (BayKliF). We acknowledge the valuable suggestions made by two anonymous reviewers which made us improve our analyses.

References

Allen, C. D., Macalady, A. K., Chenchouni, H., Bachelet, D., McDowell, N., Vennetier, M., Kitzberger, T., Rigling, A., Breshears, D. D., Hogg, E. H. (Ted), Gonzalez, P., Fensham, R., Zhang, Z., Castro, J., Demidova, N., Lim, J.-H., Allard, G., Running, S. W., Semerci, A. and Cobb, N.: A global overview of drought and heat-induced tree mortality reveals emerging climate change risks for forests, For. Ecol. Manag., 259(4), 660–684, doi:10.1016/j.foreco.2009.09.001, 2010.

Allen, C. D., Breshears, D. D. and McDowell, N. G.: On underestimation of global vulnerability to tree mortality and forest die-off from hotter drought in the Anthropocene, Ecosphere, 6(8), 1–55, doi:10.1890/ES15-00203.1, 2015.

Anderegg, W. R. L., Schwalm, C., Biondi, F., Camarero, J. J., Koch, G., Litvak, M., Ogle, K., Shaw, J. D., Shevliakova, E., Williams, A. P., Wolf, A., Ziaco, E. and Pacala, S.: Pervasive drought legacies in forest ecosystems and their implications for carbon cycle models, Science, 349(6247), 528–532, doi:10.1126/science.aab1833, 2015.

Anderegg, W. R. L., Konings, A. G., Trugman, A. T., Yu, K., Bowling, D. R., Gabbitas, R., Karp, D. S., Pacala, S., Sperry, J. S., Sulman, B. N. and Zenes, N.: Hydraulic diversity of forests regulates ecosystem resilience during drought, Nature, 561(7724), 538, doi:10.1038/s41586-018-0539-7, 2018.

Anyamba, A. and Tucker, C. J.: Historical perspective of AVHRR NDVI and vegetation drought monitoring, Remote Sens. Drought Innov. Monit. Approaches, 23, 2012.

Bastos, A., Ciais, P., Park, T., Zscheischler, J., Yue, C., Barichivich, J., Myneni, R. B., Peng, S., Piao, S. and Zhu, Z.: Was the extreme Northern Hemisphere greening in 2015 predictable?, Environ. Res. Lett., 12(4), 044016, doi:10.1088/1748-9326/aa67b5, 2017.

Beguería, S. and Vicente-Serrano, S. M.: SPEI: calculation of the standardised precipitation-evapotranspiration index. R package version 1.6., 2013.

Bigler, C., Bräker, O. U., Bugmann, H., Dobbertin, M. and Rigling, A.: Drought as an Inciting Mortality Factor in Scots Pine Stands of the Valais, Switzerland, Ecosystems, 9(3), 330–343, doi:10.1007/s10021-005-0126-2, 2006.

Breshears, D. D., Cobb, N. S., Rich, P. M., Price, K. P., Allen, C. D., Balice, R. G., Romme, W. H., Kastens, J. H., Floyd, M. L., Belnap, J., Anderson, J. J., Myers, O. B. and Meyer, C. W.: Regional vegetation die-off in response to global-change-type drought, Proc. Natl. Acad. Sci. U. S. A., 102(42), 15144–15148, doi:10.1073/pnas.0505734102, 2005.

Buras, A., Schunk, C., Zeiträg, C., Herrmann, C., Kaiser, L., Lemme, H., Straub, C., Taeger, S., Gößwein, S., Klemmt, H.-J. and Menzel, A.: Are Scots pine forest edges particularly prone to drought-induced mortality?, Environ. Res. Lett. [online] Available from: http://iopscience.iop.org/10.1088/1748-9326/aaa0b4, 2018.

Cailleret, M., Jansen, S., Robert, E. M. R., Desoto, L., Aakala, T., Antos, J. A., Beikircher, B., Bigler, C., Bugmann, H., Caccianiga, M., Čada, V., Camarero, J. J., Cherubini, P., Cochard, H., Coyea, M. R., Čufar, K., Das, A. J., Davi, H., Delzon, S., Dorman, M., Gea-Izquierdo, G., Gillner, S., Haavik, L. J., Hartmann, H., Hereş, A.-M., Hultine, K. R., Janda, P., Kane, J. M., Kharuk, V. I., Kitzberger, T., Klein, T., Kramer, K., Lens, F., Levanic, T., Linares Calderon, J. C., Lloret, F., Lobo-Do-Vale, R., Lombardi, F., López Rodríguez, R., Mäkinen, H., Mayr, S., Mészáros, I., Metsaranta, J. M., Minunno, F., Oberhuber, W., Papadopoulos, A., Peltoniemi, M., Petritan, A. M., Rohner, B., Sangüesa-Barreda, G., Sarris, D., Smith, J. M., Stan, A. B., Sterck, F., Stojanović, D. B., Suarez, M. L., Svoboda, M., Tognetti, R., Torres-Ruiz, J. M., Trotsiuk, V., Villalba, R., Vodde, F., Westwood, A. R., Wyckoff, P. H., Zafirov, N. and Martínez-Vilalta, J.: A synthesis of radial growth patterns preceding tree mortality, Glob. Change Biol., 23(4), 1675–1690, doi:10.1111/gcb.13535, 2017.

Chen, J., Franklin, J. F. and Spies, T. A.: Contrasting microclimates among clearcut, edge, and interior of old-growth Douglas-fir forest, Agric. For. Meteorol., 63(3), 219–237, doi:10.1016/0168-1923(93)90061-L, 1993.

Chen, J., Saunders, S. C., Crow, T. R., Naiman, R. J., Brosofske, K. D., Mroz, G. D., Brookshire, B. L. and Franklin, J. F.: Microclimate in Forest Ecosystem and Landscape EcologyVariations in local climate can be used to monitor and compare the effects of different management regimes, BioScience, 49(4), 288–297, doi:10.2307/1313612, 1999.

Choat, B., Brodribb, T. J., Brodersen, C. R., Duursma, R. A., López, R. and Medlyn, B. E.: Triggers of tree mortality under drought, Nature, 558(7711), 531–539, doi:10.1038/s41586-018-0240-x, 2018.

Ciais, P., Reichstein, M., Viovy, N., Granier, A., Ogée, J., Allard, V., Aubinet, M., Buchmann, N., Bernhofer, C., Carrara, A., Chevallier, F., Noblet, N. D., Friend, A. D., Friedlingstein, P., Grünwald, T., Heinesch, B., Keronen, P., Knohl, A., Krinner, G., Loustau, D., Manca, G., Matteucci, G., Miglietta, F., Ourcival, J. M., Papale, D., Pilegaard, K., Rambal, S., Seufert, G., Soussana, J. F., Sanz, M. J., Schulze, E. D., Vesala, T. and Valentini, R.: Europe-wide reduction in primary productivity caused by the heat and drought in 2003, Nature, 437(7058), 529–533, doi:10.1038/nature03972, 2005.

Fink, A. H., Brücher, T., Krüger, A., Leckebusch, G. C., Pinto, J. G. and Ulbrich, U.: The 2003 European summer heatwaves and drought –synoptic diagnosis and impacts, Weather, 59(8), 209–216, doi:10.1256/wea.73.04, 2004.

Fischer, E. M., Seneviratne, S. I., Vidale, P. L., Lüthi, D. and Schär, C.: Soil Moisture–Atmosphere Interactions during the 2003 European Summer Heat Wave, J. Clim., 20(20), 5081–5099, doi:10.1175/JCLI4288.1, 2007.

García-Herrera, R., Díaz, J., Trigo, R. M., Luterbacher, J. and Fischer, E. M.: A review of the European summer heat wave of 2003, Crit. Rev. Environ. Sci. Technol., 40(4), 267–306, 2010.

Hargreaves, G. H.: Defining and Using Reference Evapotranspiration, J. Irrig. Drain. Eng., 120(6), 1132–1139, doi:10.1061/(ASCE)0733-9437(1994)120:6(1132), 1994.

Harris, I., Jones, P. d., Osborn, T. j. and Lister, D. h.: Updated high-resolution grids of monthly climatic observations – the CRU TS3.10 Dataset, Int. J. Climatol., 34(3), 623–642, doi:10.1002/joc.3711, 2014.

Horton, D. E., Johnson, N. C., Singh, D., Swain, D. L., Rajaratnam, B. and Diffenbaugh, N. S.: Contribution of changes in atmospheric circulation patterns to extreme temperature trends, Nature, 522(7557), 465–469, doi:10.1038/nature14550, 2015.

Huete, A., Didan, K., Miura, T., Rodriguez, E. P., Gao, X. and Ferreira, L. G.: Overview of the radiometric and biophysical performance of the MODIS vegetation indices, Remote Sens. Environ., 83(1), 195–213, doi:10.1016/S0034-4257(02)00096-2, 2002.

Huete, A. R., Didan, K., Shimabukuro, Y. E., Ratana, P., Saleska, S. R., Hutyra, L. R., Yang, W., Nemani, R. R. and Myneni, R.: Amazon rainforests green-up with sunlight in dry season, Geophys. Res. Lett., 33(6), doi:10.1029/2005GL025583, 2006.

IPCC: Climate change 2014: synthesis report. Contribution of Working Groups I, II and III to the fifth assessment report of the Intergovernmental Panel on Climate Change, IPCC., 2014.

Ježík, M., Blaženec, M., Letts, M. G., Ditmarová, Ľ., Sitková, Z. and Střelcová, K.: Assessing seasonal drought stress response in Norway spruce (Picea abies (L.) Karst.) by monitoring stem circumference and sap flow, Ecohydrology, 8(3), 378–386, doi:10.1002/eco.1536, 2015.

Kalnay, E., Kanamitsu, M., Kistler, R., Collins, W., Deaven, D., Gandin, L., Iredell, M., Saha, S., White, G., Woollen, J., Zhu, Y., Chelliah, M., Ebisuzaki, W., Higgins, W., Janowiak, J., Mo, K. C., Ropelewski, C., Wang, J., Leetmaa, A., Reynolds, R., Jenne, R. and Joseph, D.: The NCEP/NCAR 40-Year Reanalysis Project, Bull. Am. Meteorol. Soc., 77(3), 437–472, doi:10.1175/1520-0477(1996)077<0437:TNYRP>2.0.CO;2, 1996.

Kannenberg, S. A., Maxwell, J. T., Pederson, N., D'Orangeville, L., Ficklin, D. L. and Phillips, R. P.: Drought legacies are dependent on water table depth, wood anatomy and drought timing across the eastern US, Ecol. Lett., doi:10.1111/ele.13173, 2018.

Klein, T.: The variability of stomatal sensitivity to leaf water potential across tree species indicates a continuum between isohydric and anisohydric behaviours, Funct. Ecol., 28(6), 1313–1320, doi:10.1111/1365-2435.12289, 2014.

Kohler, M., Sohn, J., Nägele, G. and Bauhus, J.: Can drought tolerance of Norway spruce (<Emphasis Type="Italic">Picea abies</Emphasis> (L.) <Emphasis Type="Italic">Karst</Emphasis>.) be increased through thinning?, Eur. J. For. Res., 129(6), 1109–1118, doi:10.1007/s10342-010-0397-9, 2010.

Kornhuber, K., Osprey, S., Coumou, D., Petri, S., Petoukhov, V., Rahmstorf, S. and Gray, L.: Extreme weather events in early summer 2018 connected by a recurrent hemispheric wave-7 pattern, Environ. Res. Lett., 14(5), 054002, doi:10.1088/1748-9326/ab13bf, 2019.

Li, X., Xiao, J., He, B., Arain, M. A., Beringer, J., Desai, A. R., Emmel, C., Hollinger, D. Y., Krasnova, A., Mammarella, I., Noe, S. M., Ortiz, P. S., Rey-Sanchez, A. C., Rocha, A. V. and Varlagin, A.: Solar-induced chlorophyll fluorescence is strongly correlated with terrestrial photosynthesis for a wide variety of biomes: First global analysis based on OCO-2 and flux tower observations, Glob. Change Biol., 24(9), 3990–4008, doi:10.1111/gcb.14297, 2018.

Li, Z., Li, X., Wei, D., Xu, X. and Wang, H.: An assessment of correlation on MODIS-NDVI and EVI with natural vegetation coverage in Northern Hebei Province, China, Procedia Environ. Sci., 2, 964–969, doi:10.1016/j.proenv.2010.10.108, 2010.

Matusick, G., Ruthrof, K. X., Kala, J., Brouwers, N. C., Breshears, D. D. and Hardy, G. E. S. J.: Chronic historical drought legacy exacerbates tree mortality and crown dieback during acute heatwave-compounded drought, Environ. Res. Lett., 13(9), 095002, doi:10.1088/1748-9326/aad8cb, 2018.

Misra, G., Buras, A. and Menzel, A.: Effects of different methods on the comparison between land surface and ground phenology—A methodological case study from south-western Germany, Remote Sens., 8(9), 753, 2016.

Misra, G., Buras, A., Heurich, M., Asam, S. and Menzel, A.: LiDAR derived topography and forest stand characteristics largely explain the spatial variability observed in MODIS land surface phenology, Remote Sens. Environ., 218, 231–244, doi:10.1016/j.rse.2018.09.027, 2018.

Myneni, R. B., Hall, F. G., Sellers, P. J. and Marshak, A. L.: The interpretation of spectral vegetation indexes, IEEE Trans. Geosci. Remote Sens., 33(2), 481–486, 1995.

Orth, R., Zscheischler, J. and Seneviratne, S. I.: Record dry summer in 2015 challenges precipitation projections in Central Europe, Sci. Rep., 6, 28334, doi:10.1038/srep28334, 2016.

Pfleiderer, P. and Coumou, D.: Quantification of temperature persistence over the Northern Hemisphere land-area, Clim. Dyn., 51(1–2), 627–637, doi:10.1007/s00382-017-3945-x, 2018.

Pinheiro, J., Bates, D., DebRoy, S., Sarkar, D., Heisterkamp, S., Van Willigen, B. and Maintainer, R.: Package 'nlme,' Linear Nonlinear Mix. Eff. Models Version, 3–1, 2017.

Rehschuh, R., Mette, T., Menzel, A. and Buras, A.: Soil properties affect the drought susceptibility of Norway spruce, Dendrochronologia, doi:10.1016/j.dendro.2017.07.003, 2017.

Rigling, A., Bigler, C., Eilmann, B., Feldmeyer-Christe, E., Gimmi, U., Ginzler, C., Graf, U., Mayer, P., Vacchiano, G., Weber, P., Wohlgemuth, T., Zweifel, R. and Dobbertin, M.: Driving factors of a vegetation shift from Scots pine to pubescent oak in dry Alpine forests, Glob. Change Biol., 19(1), 229–240, doi:10.1111/gcb.12038, 2013.

Robert J. Hijmans: raster: Geographic Data Analysis and Modeling., 2017.

Seneviratne, S. I., Corti, T., Davin, E. L., Hirschi, M., Jaeger, E. B., Lehner, I., Orlowsky, B. and Teuling, A. J.: Investigating soil moisture–climate interactions in a changing climate: A review, Earth-Sci. Rev., 99(3), 125–161, doi:10.1016/j.earscirev.2010.02.004, 2010.

Sippel, S., Forkel, M., Rammig, A., Thonicke, K., Flach, M., Heimann, M., Otto, F. E. L., Reichstein, M. and Mahecha, M. D.: Contrasting and interacting changes in simulated spring and summer carbon cycle extremes in European ecosystems, Environ. Res. Lett., 12(7), 075006, doi:10.1088/1748-9326/aa7398, 2017.

Team, R. C.: R: A language and environment for statistical computing, 2019.

Teuling, A. J., Seneviratne, S. I., Stöckli, R., Reichstein, M., Moors, E., Ciais, P., Luyssaert, S., van den Hurk, B., Ammann, C., Bernhofer, C., Dellwik, E., Gianelle, D., Gielen, B., Grünwald, T., Klumpp, K., Montagnani, L., Moureaux, C., Sottocornola, M. and Wohlfahrt, G.: Contrasting response of European forest and grassland energy exchange to heatwaves, Nat. Geosci., 3(10), 722–727, doi:10.1038/ngeo950, 2010.

Thornthwaite, C. W.: An Approach toward a Rational Classification of Climate, Geogr. Rev., 38(1), 55–94, doi:10.2307/210739, 1948.

Vicca, S., Balzarolo, M., Filella, I., Granier, A., Herbst, M., Knohl, A., Longdoz, B., Mund, M., Nagy, Z., Pintér, K., Rambal, S., Verbesselt, J., Verger, A., Zeileis, A., Zhang, C. and Peñuelas, J.: Remotely-sensed detection of effects of extreme droughts on gross primary production, Sci. Rep., 6, 28269, doi:10.1038/srep28269, 2016.

Wolf, S., Eugster, W., Ammann, C., Häni, M., Zielis, S., Hiller, R., Stieger, J., Imer, D., Merbold, L. and Buchmann, N.: Contrasting response of grassland versus forest carbon and water fluxes to spring drought in Switzerland, Environ. Res. Lett., 8(3), 035007, doi:10.1088/1748-9326/8/3/035007, 2013.

Xu, L., Samanta, A., Costa, M. H., Ganguly, S., Nemani, R. R. and Myneni, R. B.: Widespread decline in greenness of Amazonian vegetation due to the 2010 drought, Geophys. Res. Lett., 38(7), doi:10.1029/2011GL046824, 2011.

Young, A. and Mitchell, N.: Microclimate and vegetation edge effects in a fragmented podocarp-broadleaf forest in New Zealand, Biol. Conserv., 67(1), 63–72, doi:10.1016/0006-3207(94)90010-8, 1994.

Zang, C. S., Buras, A., Esquivel-Muelbert, A., Jump, A. S., Rigling, A. and Rammig, A.: Standardized drought indices in ecological research: Why one size does not fit all, Glob. Change Biol., n/a(n/a), doi:10.1111/gcb.14809, 2019.

Zscheischler, J. and Seneviratne, S. I.: Dependence of drivers affects risks associated with compound events, Sci. Adv., 3(6), e1700263, doi:10.1126/sciadv.1700263, 2017.

Zscheischler, J., Westra, S., van den Hurk, B. J. J. M., Seneviratne, S. I., Ward, P. J., Pitman, A., AghaKouchak, A., Bresch, D. N., Leonard, M., Wahl, T. and Zhang, X.: Future climate risk from compound events, Nat. Clim. Change, 8(6), 469–477, doi:10.1038/s41558-018-0156-3, 2018.

Public news references

https://www.climate.gov/news-features/event-tracker/hot-dry-summer-has-led-drought-europe-2018 (in English).

https://www.euronews.com/2018/08/10/explained-europe-s-devastating-drought-and-the-countries-worst-hit (in English).

Short-term outlook of the European Commission for EU agricultural markets: https://ec.europa.eu/agriculture/markets-and-prices/short-term-outlook_en (in English).

MODIS-based maps on land surface temperature and cloud cover anomalies for whole Europe: https://www.geografiainfinita.com/2018/09/un-analisis-de-la-sequia-en-europa-en-el-verano-de-2018/?platform=hootsuite (in Spanish).

German atlas for soil water depletion, provided by the Umwelt-Forschungs-Zentrum UFZ: https://www.ufz.de/index.php?de=44429 (in German).

Report on the impacts of the heat-wave in Germany, provided by the Karlsruhe Institute of Technology KIT: http://www.kit.edu/kit/pi_2018_102_durre-betrifft-rund-90-prozent-der-flache-deutschlands.php (in German).

~~Interim report of ‚Wald und Holz NRW' on the impacts of the drought 2018 on forest productivity in North Rhine Westphalia: https://www.wald-und-holz.nrw.de/aktuelle-meldungen/2018/zwischenbilanz-trockensommer-2018 (in German).~~

BMEL, 2019: Deutschlands Wald im Klimawandel – Eckpunkte und Maßnahmen (in German). Published by the Federal Ministry of Food and Agriculture, Germany.

Pictures from dried-out cornfields in Germany: https://www.alamy.com/corn-field-dried-up-and-only-grown-low-small-corn-cobs-through-the-summer-drought-drought-in-ostwestfalen-lippe-germany-summer-2018-image215773502.html

Report on early leaf shedding of deciduous trees in Germany: https://www.wetteronline.de/wetternews/trockenheit-setzt-natur-zu-viele-baeume-werfen-ihr-laub-ab-2018-08-14-lb (in German)

New insights on the impacts of the drought 2018 in Switzerland: https://www.wsl.ch/de/ueber-die-wsl/programme-und-initiativen/wsl-initiative-trockenheit-2018/c2-gruen-waldbedachung.html (in German).

Beech die-back in the Hainich national park in Germany: https://www.nationalpark-hainich.de/de/aktuelles/aktuelles-presse/einzelansicht/extremjahr-2018-hinterlaesst-spuren-im-nationalpark-hainich.html (in German).

Report on the state of German forests in ZEIT online (in German): https://www.zeit.de/2019/35/duerre-waldsterben-klimawandel-massnahmen-foersterei